FLUORESCENCE-BASED SENSING MATRICES FOR HEAVY METAL DETECTION IN WATER, SPOILAGE MONITORING AND UREA DETECTION IN MILK

M.Sc. Thesis

By
AKSHAY MEHTA

DEPARTMENT OF BIOSCIENCES AND BIOMEDICAL ENGINEERING
INDIAN INSTITUTE OF TECHNOLOGY INDORE

FLUORESCENCE-BASED SENSING MATRICES FOR HEAVY METAL DETECTION IN WATER, SPOILAGE MONITORING AND UREA DETECTION IN MILK

A THESIS

Submitted in partial fulfillment of the requirements for the award of the degree
of
Master of Science

by
AKSHAY MEHTA

DEPARTMENT OF BIOSCIENCES AND BIOMEDICAL ENGINEERING
INDIAN INSTITUTE OF TECHNOLOGY INDORE

May 2022

INDIAN INSTITUTE OF TECHNOLOGY INDORE

CANDIDATE'S DECLARATION

I hereby certify that the work which is being presented in the thesis **FLUORESCENCE-BASED SENSING MATRICES FOR HEAVY METAL DETECTION IN WATER, SPOILAGE MONITORING AND UREA DETECTION IN MILK** in the partial fulfilment of the requirements for the award of the degree of **MASTER OF SCIENCE** and submitted in the **DEPARTMENT OF BIOSCIENCES AND BIOMEDICAL ENGINEERING, Indian Institute of Technology Indore**, is an authentic record of my own work carried out during the time period from August 2020 to May 2022 under the supervision of **Dr Abhijeet Joshi**, Associate professor, Department of Biosciences and Biomedical Engineering, IIT Indore.

The matter presented in this thesis has not been submitted by me for the award of any other degree of this or any other institute.

27 May 2022
(AKSHAY MEHTA)

This is to certify that the above statement made by the candidate is correct to the best of my knowledge.

Signature of the Supervisor

Dr Abhijeet Joshi

AKSHAY MEHTA has successfully given his M.Sc. Oral Examination held on **05 May, 2022**.

Signature(s) of Supervisor(s) of MSc thesis
Date: 27-05-2022

Convener, DPGC
Date: 05-05-2022

Signature of PSPC Member #1
Date: 27-05-2022

Signature of PSPC Member #1
Date: 05-05-2022

Acknowledgement

This project would not have been possible without the support of many people. It gives me great joy and pleasure to acknowledge them.

I would like to express my gratitude to my project supervisor and guide, **Dr Abhijeet Joshi**, for allowing me to work in his lab. From research techniques to life lessons in his lab, I learned many new things in his lab. His scientific guidance and advice continuously helped to move things further. I want to thank him for finding time in his busy schedule to discuss the ideas and results with me. His personality will always inspire me.

I would like to thank my PSPC members, **Prof. Prashant Kodgire** and **Dr Parimal Kar**, for their valuable suggestions during the project's progress. I like to thank **Prof. Amit Kumar** (HoD, BSBE**), Prof. Prashant Kodgire** (DPGC convenor) and **Dr Parimal Kar** (course coordinator).

I extend my gratitude to all faculty members of BSBE, IIT Indore, for teaching me new research techniques. I would like to thank **Prof. Suhas Joshi** (Director, IIT Indore) for allowing me to be a part of this eminent institute.

I want to thank the BSBE department and SIC, IIT Indore, for the instrumentational facilities.

A heartful thanks to my senior lab member **Dr Sandeep Chaudhary.** Throughout the project, he guided and helped me clear my doubts. I am grateful to my other senior lab members, **Mr Tanmay Vyas** and **Miss Surbhi Jaisal**.

Further, I would like to thank my family away from home, Mr Ankit Jaiswal, Mr Krishna Singh, Mr Rahul Chaudhary, Miss Kanika Singh and Mr Brijeshwar Singh.

A special thanks to my friend Vedant Salve for all the laughs and love.

Most importantly, I have deep gratitude to my mother, Maya Devi, for her unconditional love, support and care. I can not imagine any god without her.

Abstract

The first objective of this study is the detection of heavy metal ions in water using fluorescent Carbon Quantum Dots. Carbon Quantum Dots are carbon nanoparticles (size around or less than 10nm) that show fluorescence upon excitation with a light of a particular wavelength. Heavy metal ions behave as quenchers when they come in contact with Carbon Quantum Dots. The degree of quenching is directly proportional to the heavy metal concentration in the sample (in the concentration range of 0-100μM). Using this phenomenon, the presence or concentration of heavy metals can be determined. Heavy metals like Mn, Pb, Ni, Co, Hg and Cr showed a linear relationship between the heavy metal ion concentration in the solution phase and the fluorescence intensity of Carbon Quantum Dots. Same beavious is observed in Carbon Quantum Dot embedded thin film also. The study reports the developmental a fluorescence based thin that cat detect heavy metal ion ceoncemtration in water.

The second objective of this study is the detection of mil spoilage and urea adulteration using recombinant mTFP. mTFP is a fluorescent protein that shows pH sensitivity. The change in pH leads to a change in the fluorescence intensity of the protein. This property is used to detect milk spoilage. When mixed with the urease enzyme, urea adultered milk shows a rapid pH change. This pH change causes a change in the fluorescence intensity of mTFP and is detected by the fluorescence reader. This study reports urea detection in milk in the range of 0-100mM.

Keywords: Carbon Quantum Dots. Pollution, heavy metal toxicity, heavy metal detection, fluorescence-based sensor, fluorescence quenching, mTFP, urea adulteration, milk pH.

Contents

List of figures

List of tables

Abbreviations

TED	Triethylenediamine
XRD	X-ras Diffraction
FTIR	Fourier Transform Infrared Spectroscopy
CQDs	Carbon Quantum Dots
FITC	Fluorescein isothiocyanate
TRITC	Tetramethylrhodamine-isothiocyanate
FDA	Fluorescein diacetate
AQI	Air Quality Index
GIT	Gastrointestinal Tract
CCD	Charge-coupled device
LED	Light Emitting Diode
UV	Ultraviolet
LOD	Limit of detection
LOQ	Limit of quantification

1. Chapter 1 Introduction

In recent years, fluorescent chemical sensors and bio-sensors have caught the attention of scientists due to their high sensitivity, high specificity, immune to light scattering, and ease of operation. They have a wide variety of applications in food and healthcare monitoring. Fluorescent sensors interact with the analyte and produce a signal detected by the detector. Any change in the analyte concentration leads to a change in the signal of fluorescent signal. Some fluorescent sensors show pH-sensitive properties and hence can be used as pH sensors. They are more accurate and easy to use. The first objective of this study focuses on developing fluorescent sensors to detect heavy metal ions in water. The second object is to detect the natural spoilage and urea adulteration in milk

1.1. The problem of pollution

The industrial revolution started in the last decades of the 18th century has proved as a boon to the world. It provided countless opportunities to the world and individuals. It began in the factories, but today its impact can be seen in every street and household. The Industrial Revolution brought jobs and technologies to the world, and the most significant problem of the upcoming centuries- pollution. However, pollution existed before the industrial revolution as natural pollution, but its impact on the environment was not significant. Human activities increased it drastically. The pollution problem has become so big that several animal species are extinct, and now the danger is on the existence of the human species. A pollution causing agent or pollutant is generally defined as a substance that creates disturbances or undesirable changes in the natural structure of the environment. Unfortunately, the number of these substances is increasing year by year[1].

Recently, India's one of the most polluted cities, Delhi, has witnessed a highly increased rate of AQI that the government had to imply a lockdown to reduce traffic on roads.

1.2. Heavy metal pollution

Metal ions with high relative mass and density are more toxic and potential pollutants for the environment[2]. However, toxicity is more concerned with the chemical reactivity than the mass and density[3] the major contributing

elements in heavy metal pollution are Mercury (Hg), Lead (Pb), Manganese (Mn), Nickel (Ni), Cobalt (Cr), Chromium (Cr), Cadmium (Cd) and Arsenic (As). Primary sources of these heavy metal ions are smelting, mining and industrial waste materials. Heavy metal ions pollute surface water, soil and food products. Through leaching, heavy metals from landfills and water dumps reach the groundwater. Polluted water sources can affect human health and the economy of the nation. Heavy metals show lasting effects in the environment as they are non-biodegradable. The primary reason for heavy metal ions toxicity in a biosystem is their reactivity with thiol groups in the proteins[4]. Also, they alter the biochemical activities inside the cell environment[5,6]. Metals like Aluminium and Copper are also becoming a significant threat. Due to the regular use of Aluminium foil for food packing and Aluminium and Copper utensils for cooking purposes, we are now more susceptible to consuming these metal ions. After a certain consumption limit, metal ions also show toxic effects in the body. One significant toxic effect is that they inhibit enzyme activities[7].

Table 1.1 Toxic effects of heavy metal ions on the human body8

Metal ion	**Major sources**	**Effects on health**	**Permissible limit (mg/l)**
Hg	Mercury-containing pesticides, non-rechargeable batteries.	Can damage the digestive system, lungs, skin and nervous system, irritability, fatigue	0.01
As	Pesticides, natural/ore deposits, mining industries	Poisoning can affect the lungs, skin and digestive system	0.02

Pb	Paint, pesticide, smoking, automobile emission, mining, burning of coal	Mental retardation in children, developmental delay, fatal infant encephalopathy, congenital paralysis, sensor neural deafness and, acute or chronic damage to the nervous system, epilepticus, liver, kidney, gastrointestinal damage	0.1
Al	Household utensils, food Packing foil, aluminium pipes	Anaemia, lung-related diseases, bone-related diseases	2700
Cu	Metal pipes, cooking utensils, mining, electronic durables	GIT related issues, anaemia, liver and kidney damage	0.1
Mn	Steel and iron industries, ore deposits	Can damage the nervous system, tremors	0.26
Cr	Mining industries, mineral deposits	Cement duts, landfills	0.05
Cd	Welding, electroplating, pesticide fertilizer, Cd and Ni batteries, nuclear fission plant	Can damage lungs, bones, nervous system, kidney, circulatory and digestive system	0.06

1.3. Detection of Heavy metal ions

Heavy metal ions are very toxic, and their removal from consumable materials is necessary. Once they enter the food chain, they get accumulated in the alimentary chain[9]. Prior to removal, detection of these ions in the sample is crucial. For this purpose, spectroscopic, chromatographic and electronic methods are popular and valuable. Scientists have reported the methods to detect heavy metal ions using High-performance liquid chromatography (HPLC)[10]; surface-enhanced Raman scattering (SERS)[11], x-ray absorption spectroscopy[12], Atomic Absorption Spectroscopy (AAS)[13], electroanalytical methods[14] and colourimetric methods[15] successfully.

Flavio M. Shimizu et al. reviewed the applicability of electroanalytical methods for heavy metal detection[16]. However, these analytical methods require a skilled workforce and are time-consuming. Fluorescence-based techniques are relatively more straightforward and a little time-consuming.

1.4. Chemical sensors

A chemical sensor device/instrument/setup results from the combined application of chemistry, physics, and computer science and is designed for chemical recognition[17]. When the sensors interact with the analytes, it produces a signal. The signal recognized by the instrument can be a chemical, electrical, physical or optical signal. This signal contains information about the presence or concentration of the analyte. Any change in the intensity of the signal is in proportion to a change in the analyte's concentration, and by measuring this change, analyte concentration can be judged.

1.5. Fluorescence-based sensors

Fluorescence-based methods are emerging in the field of analyte sensing. Fluorescence-based sensors come under the category of optical sensors because the signal detected by these sensors is light. When the concentration of the sample changes, fluorescence intensity also changes. Fluorescent dyes like FITC, TRITC, Fluo-4, FDA etc., are the most common in this field, but quantum dots seem to replace them soon. Quantum dots are synthetic nanoparticles that show fluorescence properties. Quantum dots are categorized based on their precursor materials. Metal-based quantum dots

(MQDs), graphene quantum dots, carbon nanodots and Carbon Quantum Dots are gaining popularity in application-based fields[18]. Compared with dyes, Carbon Quantum Dots are less toxic, biocompatible, easy to prepare, have good photostability, and are environment friendly[19]. They are helpful for environmental monitoring, food quality assessment and healthcare. In food quality assessment, the usefulness of Carbon Quantum Dots is reported. Hanzhi Fan et al. published a review article regarding the synthesis of Carbon Quantum Dots (CQDs) from food waste material and its use in food quality assessment[20].

Carbon Quantum Dot as a biosensor is relatively new to the scientific community, and much research is yet to be done on it. It has the potential to be useful for numerous applications in the future. Great efforts are making the Carbon Quantum Dots a promising biosensor. More transformations and modifications will undoubtedly increase their applicability and use in the field of bioimaging[26], cell labelling[27], photodynamic therapy[28], drug delivery[29,30] biosensing[31,32]. Ying Lim et al. summarized the applications of Carbon Quantum Dots[3]

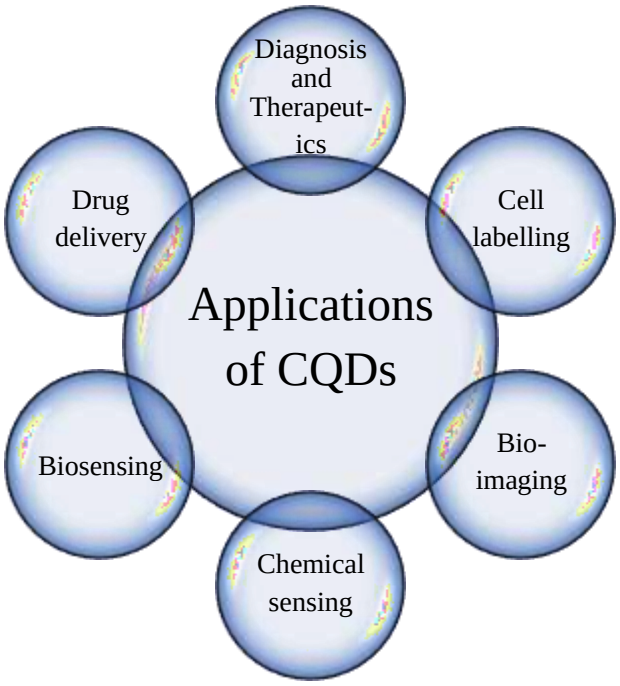

Figure 1.1 Applications of CQDs

1.6. Fluorescence mechanism in a Carbon Quantum Dot molecule

The complete electronic mechanism by which the Carbon Quantum Dot molecules give fluorescence is yet to be understood. However, many researchers have a proposed mechanism or theory. Some of them have reported that the oxygenated functional groups found on the surface of carbon quantum dot molecules are responsible for the fluorescence properties of CQDs[34]. It is hypothesized that excitation of charge carriers in CQDs by light/photos and channelling from valence band to conduction band release energy as photos. These emitted photons are observed as fluorescence[35]. Surface functional groups act as trap site sites for photoexcited electrons. When these function groups interact with heavy metal ions through coordination or electrostatic interaction chemistry, the excited electron comes to the ground state without emitting photons[36]. This phenomenon is observed as fluorescence quenching[37].

1.7. Carbon quantum dot synthesis methods

Till now, scientists have reported numerous methods to synthesize Carbon Quantum Dots[38]. Carbon quantum dot provides the flexibility to use any compound as a precursor and method from the reported methods according to the availability of resources. However, some of the properties of CQDs

can be affected by their preparation method and starting material. Polycyclic aromatic hydrocarbons are used in most of the methods[20]. However, the green synthesis of CQDs using plant and animal products is also getting the attention of scientists[33]. In this study, TED and Phthalic Acid were used as precursors of Carbon Quantum Dots.

1.8. The problem of spoilage and adulteration in milk

Milk is considered a complete food because it contains almost all the nutrients required for the normal growth of the human body. Still, one of the biggest problems associated with milk is that it can not be stored at room temperature for a longer duration. Natural spoilage of milk is a big hurdle in the processing and shipping of milk. With time the *lactobacillus* bacteria grow in milk and utilize the lactose by converting it into lactic acid. When lactic acid concentration increases, the pH of milk decreases. The change in milk pH is a great indicator of spoilage[39]. One of the most used methods to measure pH is by pH meter. However, less accuracy is a concern associated with detecting pH by a pH meter. The pH fluctuates while observing; hence it's not easy to get a stable signal. Apart from this, a pH meter requires regular maintenance and frequent calibration. The pH meter electrode is made up of glass and pores on its diaphragm at the end. Any blockage to these pores can be inaccessible to the solution and, hence, wrong measurement. Also, the resolution of a pH meter is not very good. On the other hand, a pH-sensitive fluorescent element can detect a minor change in the pH. It shows a change in the fluorescent intensity when pH changes.

Monomeric teal fluorescent protein or mTFP is a 27kDa protein that shows fluorescence when exposed to 462nm light. The emission peak observed is at 492nm. It shows a change in the emission intensity when exposed to different pH conditions[40]. The pH of fresh and unspoiled milk is around 6.5-6.7 (slightly acidic). With time, lactic acid concentration increases and pH can decrease up to 4. The fluorescence of mTFP shows a good sensitivity in this range, so it will be used t detect milk pH in this study.

The second problem associated with milk is urea adulteration. Urea is mixed in the milk to increase its whiteness consistency and delay the natural spoilage process. When urea adultered milk is added with urea enzymes, the urea gets degraded, and ammonium ions are produced. Ammonium ions are

responsible for the increase in the pH of the reaction mixture. The increase in the pH due to the urea-urease reaction is directly related to urea concentration in milk. Hence, by detecting the pH change, we can determine the urea concentration in milk with the help of mTFP.

2. Chapter 2 Material and Methods

2.1. Materials

Phthalic acid (MW 166.14 g/mol), Nickel(II) chloride hexahydrate (MW 129.59g/mol), Lead (II) chloride (MW 278.11 g/mol), Manganese (II) chloride tetrahydrate (MW 197.91), Chromium (III) chloride (MW 266.45g/mol), Cobalt (II) Chloride hexahydrate (MW 118.965 g/mol), Mercury (II) Chloride (MW 271.50 g/mol), and triethylenediamine (TED; MW 112.17 g/mol) were procured from Sigma-Aldrich India and used as received without any further purification. Agarose powder special low EED was obtained from HiMedia. Deionized water was used to synthesize Carbon Quantum Dots and prepare all aquatic solutions and buffers for the experiment.

For milk sensing studies, mTFP cloned pET28a was obtained from Prof. Prashant Kodgire's lab (BSBE, IIT Indore). Urea powder, Lysozyme, Tris-Cl, Bis-Tris propane buffer, Imidazole, and NaCl were purchased from Sigma-Aldrich India. Urease enzyme (Crystalized, extracted from JackBean) was bought from HiMedia.

2.2. Experimental setup for heavy metal studies

2.2.1. Components

Optical fibre cable and copper wires for connections were bought from Amazon (India). A cuvette holder was designed and 3-D printed locally (with dimensions of W × L × H:: 4 cm× 4 cm× 4.5 cm). A Samsung microwave oven is used for the synthesis of CQDs. All components were already in use without any modifications for scientific studies.

2.2.2. Details and Working mechanism of the Sensing Instrument (Optical Fibre Spectrophotometer)

A though hole UV-LED (λ =365) lamp was purchased from Thor Lab USA and used as a light source to excite Carbon Dots. The LED was connected directly to the 3D-printed cuvette holder. A quartz cuvette (1 cm path length) was used for fluorescence observations. The fluorescence emission spectra for pH sensing were observed on an optical fibre spectrometer (OFS) device (purchased from Ocean Optics, USA). The spectrometer was

built-in with a photodetector. The photodetector was connected to the cuvette holder orthogonal to the light source with a connecting wire and optical fibre cable. The orthogonal position of the light source and detector is to avoid the detection of exciting light by the photodetector. All The data were recorded on a computer with the software provided with the OFS instrument. Figure 1 and 2 depicts the experimental setup of the OFS device.

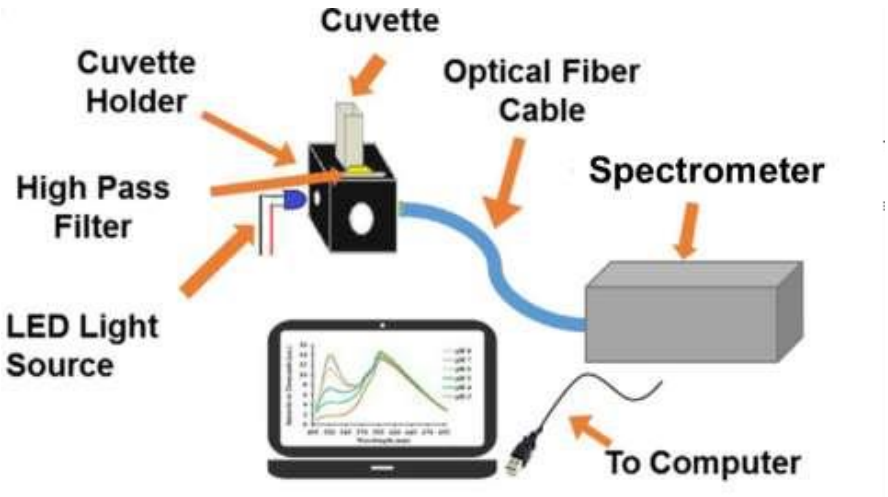

Figure 2.1 Schematic representation of OFS

Figure 2.2 Instrumental setup of OFS

2.3. Carbon Quantum Dots synthesis and characterization

2.3.1. Synthesis of CQDs

Carbon Quantum Dots were synthesized using Phthalic acid and TED in the feed ratio 1:1 (1 g of Phthalic acid and 1 g of TED were added to 3 mL of Deionized water). The mixture was stirred on a magnetic stirrer until get dissolved. The prepared solution was placed in the microwave oven at 800 W for 60 sec, where it was exposed to electromagnetic radiation in the microwave frequency range. After 60 sec, the solution colour changed from transparent to fluorescent orange. The synthesized crude product was allowed to cool down at room temperature and then passed through a 0.22-micrometre filter. The filtered solution was dialyzed in 50ml deionized water (Molecular weight cutoff ~ 14 kDa) and lyophilized for 5 hours to obtain the powder form.

2.3.2. Characterization of CQDs

To check the optical properties of CQDs, the absorbance and fluorescence spectrum were measured. The absorbance spectrum was measured using a spectrophotometer, and the fluorescence spectrum was taken using an Optical Fibre Spectrometer. Crystal structure related characterization was done with XRD. The D-spacing value and crystalline phase of the synthesized CQDs were checked. The analysis was performed using an X-ray diffractometer with Cu Xrays ($\lambda = 1.540$ Å) (Sophisticated Instruments Centre, IIT Indore)**.** The optical properties of CQDs were observed using an OFS (Ocean Optics, USA) and a UV−vis spectrometer (UV-1900i, Shimadzu, Japan). The chemical properties of lyophilized CQD powder were studied by Fourier transform infrared spectroscopy (FTIR) (Tensor 27, Bruker, Germany) in the range 4000−400 cm^{-1}.

2.3.3. Calculation of quantum yield of synthesized quantum dots

A fluorophore gets excited by the light of a suitable wavelength and emits higher wavelength light. The efficiency in converting the absorbed light into emitted light is termed quantum yield. The quantum yield is calculated by comparison with another fluorophore of known quantum yield. The quantum yield of CQDs was calculated by taking Fluorescein as a reference.

Fluorescein shows excitation at 488nm and emits the light of 521nm. The quantum yield of Fluorescein is 0.792. The Fluorescein solution was dissolved in 0.1M NaOH and diluted until the absorbance value of 0.125 was achieved.

In the same way, CQD powder is dissolved in water and diluted until the same absorbance value is achieved. At this concentration, the fluorescence of both solutions was observed. The quantum yield of CQD was calculated using the following formula-

$$Q_s = Q_R \times \frac{I_S}{A_s} \times \frac{A_R}{I_R} \times \frac{\eta_s}{\eta_R}$$

Where Q_S is the Quantum yield of CQDs,

Q_R is the quantum yield of Fluorescein,

I_S is the fluorescence intensity of CQDs,

I_R is the fluorescence intensity of Fluorescein,

A_S is the absorbance value of CQDs,

A_R is the absorbance value of Fluorescein,

And η refers to the refractive index of the solvent.

Here, the refractive index of the sample solution and reference solution is the same (η = 1.33). The concentration is optimized to keep the absorbance value the same so that the amount of light absorbed by both the samples is also the same.

2.3.4. Photostability of CQDs

The carbon quantum dost solution was stored in the dark, and its photostability was tested for 22 days. A temperature-dependent study is also done to check the effect of temperature on the fluorescence of the carbon dots. For that, the carbon dot solution was kept in a preheated block at a set temperature for about 5 minutes, and then a fluorescence signal was observed. The fluorescence signal was recorded from 30ºC to 80ºC in a 5ºC gap.

2.4. Heavy metal ion sensing by CQD solution

2.4.1. Preparation of calibration curves for different heavy metal ions

After dialysis and suspension in distilled water, the synthesized carbon quantum dot solution was ready for sensing. 500µM stock solutions of

Nickel(II) chloride hexahydrate (MW 129.59g/mol), Lead (II) chloride (MW 278.11 g/mol), Manganese (II) chloride tetrahydrate (MW 197.91), Chromium (III) chloride (MW 266.45g/mol), Cobalt (II) Chloride hexahydrate (MW 118.965 g/mol), Mercury (II) Chloride (MW 271.50 g/mol) were prepared in deionized water. From the stock solution, dilutions of 5 µM, 10 µM, 15 µM, 20 µM, 30 µM, 50 µM, 70 µM and 100 µM were prepared. Deionized water without heavy metal salts was used as a control in every experiment. A total of 3ml samples for every concentration were prepared, which contained 90 µL of CQD solution (30 µL/ml). This concentration was optimized by repeating the experiment with different concentrations of CQD solution to minimize the requirement of CQD solution without affecting the efficacy of the method/instrument.). After adding all components, the solution was mixed with a vortex mixer for about 10 sec. Before taking fluorescence observations, the mixture was kept at room temperature for 30 sec. All samples were prepared in triplicates and scanned for fluorescence observations by OFS. Analytical parameters (linearity, sensitivity, limit of detection and resolution) were evaluated using the observations. Before taking the observations in OFS, the pH of all samples was checked to make sure that heavy metal salts were not causing effects on solution pH. CQDs also show pH-sensitive properties, and it is necessary to make sure pH is not changing with the change in the concentration of heavy metal salts.

2.4.2. Analytical parameters of calibration curves.

a. **Linearity-** Mathematically, linearity is a function of values that can be graphically represented as a straight line. Linearity of an analytical method can be explained as its capability to show "results that are directly proportional to the concentration of the analyte in the sample". **(regression line)**

b. **Limit of detection or LOD** of an individual analytical procedure is the lowest amount of analyte in a sample which can be detected but not necessarily quantified as an exact value.

$$LOD = 3.3 * \frac{Standard\ deviation\ of\ lowest\ point}{Slope/sensitivity}$$

c. **Limit of quantification or LOQ** of an individual analytical procedure is the lowest amount of analyte in a sample, which can be quantitatively

determined and quantified with accuracy.

$$LOQ = 3*LOD$$

d. **Sensitivity-** Minimum detectable response generated by the change in the concentration. **(**slope**)**

e. **Resolution-** Minimum concentration difference detected by the analytical method.

$$\text{Resolution} = \frac{Standard\ deviation\ (of\ lowest\ point)}{Slope/sensitivity}$$

f. **Percentage recovery-** A ratio of predicted value and actual value (in %)

$$\%\ \text{Recovery} = \frac{Predicted\ value}{Actual\ value} \times 100$$

2.4.3. Spike and recovery studies

Spike and recovery studies are done to check the accuracy of the calibration curves. For this purpose, a known heavy metal ion concentration is introduced to the CQDs solution, and the signal is checked. The observed signal intensity is used to predict the heavy metal ion concentration in the solution with the help of the calibration curve. The predicted concentration is compared with the actual concentration, and recovery is checked. The recovery percentage value shows the accuracy and error of the calibration curve. CQDs solution was mixed with the heavy metal salt solution in a 30 µL/ml concentration. From the stock of heavy metal salt solution, dilutions of 5 µM, 10 µM, 15 µM, 20 µM, 30 µM, 50 µM, 70 µM and 100 µM were prepared. A 3ml sample for every concentration was also prepared in tap water for this study. pH is checked before every observation. Observed data were analyzed to calculate the % recovery. All observations were taken at room temperature.

2.5. Thin-film synthesis and characterization

CQDs containing thin film is ready to use solution to detect the heavy metal ions in water. For the preparation of a CQD embedded thin film, 20% (w/v) Gelatin solution was prepared and heated until a clear and transparent solution appeared. 20% Glycerine (v/v) was added to the solution. Glycerine provides water repellent property to the thin film, showing good stability in water. After that, it was allowed to cool down for some time and added with

CQDs solution in the ratio of 1:10. The Gelatin solution containing CQDs was spread on a glass plate and allowed to air dry at room temperature. Small pieces of the thin film were cut with the help of a hole puncture that is used to make holes in paper. The diameter of the thin film was 4.5mm. The dried thin film was then checked with a microplate reader to observe the fluorescence signal. A piece of the thin film was kept in one of the wells of 96 well plate and sent in the plate reader to be read. To observe the changes in the chemical composition, the FTIR spectrum of the synthesized thin film was taken. For FTIR spectroscopy, the wavelength range 4000−400 cm^{-1} is considered. XRD spectroscopy was done to analyze the crystalline structure of the thin film. The thin film was excited with 365nm UV light.

When dipped in water, the thin leaches the surface carbon dots in water because they are relatively loose bound. The thin film was dipped in water for 2 seconds, and then its fluorescence signal was observed. This process was repeated until it started giving a stable signal. The thin film was stored in the dark, and its photostability was checked for three weeks.

2.6. Heavy metal sensing with thin film

the synthesized thin film was used to determine the heavy metal ion concentration in water. First, calibration cures were prepared for all six heavy metals that showed quenching in solution phased carbon dots. For that purpose, metal salt (chloride) solutions of different concentrations were prepared (range 0-100µM). A piece of the thin film was dipped in the solution and observed for fluorescence signal. Spike and recovery studies were done to check the validity of the calibration curves with a thin film. A known concentration is introduced into tap water; then, a thin film is dipped, and the fluorescence signal is checked. The observed signal is used to predict the heavy metal ion concentration with the help of the calibration curve. Predicted and actual concentrations were compared to determine the error and accuracy of the method.

2.7. Statistical analysis

All statistical analysis was done in Microsoft Excel. In the preparation of calibration curves, the R^2 value shows the linearity of the method. Observations that have $R^2 > 0.95$ can be considered linear. The

correlation coefficient shows the relationship between two variables; fluorescence intensity and metal ion concentration, in this case.

2.8. Milk sensing with mTFP

2.8.1. mTFP induction and purification

mTFP gene cloned pET28a containing *Escherichia Coli* Rossetta (BE3) were grown in LB liquid growth media with 10µg/ml kanamycin for about 16 hrs at 37°C (220rpm) in an incubator shaker. For secondary culture, a fresh LB liquid media containing 10µg/ml kanamycin was inoculated with primary culture and kept at 37°C in an incubator shaker (220rpm) until OD 0.6 was achieved. Then, for induction of protein expression, IPTG was added in 0.1M concentration and incubated for 16 hrs at 20°C in an incubator shaker at 180 rpm. Cells were then palleted down using a centrifuge at 11000 rpm for 10 minutes. The cell pellet was then rinsed and resuspended in resuspension buffer containing Tris buffer (pH 7.4) and 10% glycerol. Cells were then lysed by adding lysozyme enzyme (400µg/ml). Cell solution with enzyme was then allowed to incubate at 30°C for 20 minutes. After incubation with enzyme, cell solution was sonicated and centrifuged at 12000 rpm for 10 minutes. Pallet and supernatant were collected in separate tubes. To determine the protein fraction in supernatant and pallet, samples were loaded on 12% SDS gel.

For purification of mTFP, the soluble fraction was selected and proceeded. As the recombinant protein contains an N-terminal 6-His tag, we used Ni-nitrilotriacetic acid column-based affinity chromatography for purification (gravity-based column). The column was pre-equilibrated with equilibration buffer (50mM Tris-Cl buffer, pH 8.0, 500mM NaCl, 20mM Imidazole). After equilibration, the column was washed with wash buffer (50mM Tris-Cl, pH 8.0, 500mM NaCl and 50mM Imidazole), and flow-through was collected. After washing, the solution was eluted with elution buffer (50mM Tris-Cl, pH 8.0, 500mM NaCl and 300 Imidazole). To check the purification of the protein, samples were run with a 12% SDS gel.

2.8.2. Bradford assay for protein estimation

2.8.3. Milk sensing studies with mTFP (solution phase)

a. To check the pH sensitivity of mTFP, the purified protein solution was

mixed with different pH buffers and checked in a microplate reader (Common instruments facility, BSBE, IIT Indore). 90µl pH buffer was added with 10µl 10x diluted protein solution, making the buffer: protein = 1:100 (total reaction volume was 100µl). All pH buffer solutions were prepared using 0.1M Citric Acid and 0.1M Sodium Citrate. The pH range considered was from 3 to 7.5 with the step of 0.5. Protein and pH buffer solution was taken in a 96 well microplate and placed in a microplate reader at room temperature. All of the pH buffer mixtures were observed simultaneously. Response time was about 10 sec to get a stable signal. A pH calibration curve was prepared with the help of fluorescence intensities observed at different pH.

b. A pH spike and recovery study was performed to check the validity and applicability of the calibration curve. For this purpose, milk and different pH buffers were mixed in a ratio of 1:3. 90µl from every mixture was transferred to a microplate and added with 10µl of 10x diluted mTFP solution. The observed fluorescence intensity is used to predict the pH with the help of a calibration curve. The predicted and actual pH were compared to calculate the % recovery and error.

c. For urea sensing, initial experiments were performed in water to produce and check the signal. In a total 100µl reaction, 500mM stock solution of urea, 15µl of freshly prepared 2mg/ml urease was added. pH 4 buffer (Acetic acid-Sodium acetate) was used to make up the volume up to 100µl. For this study, the range of considered urea concentration is from 0mM to 200mM (0mM, 10mM, 20mM, 30mM, 50mM, 70mM, 100mM and 200mM). The reaction mixture was then allowed to incubate for 5 min at 30°C. After that, the pH of the solution is checked and mixed with 10µl 10x diluted mTFP protein. 96 well plate was placed in a microplate reader to observe the fluorescence. The response time to get a stable signal for urea detection (that includes incubation time) was around 6 min. The observed fluorescence signal for different urea concentrations is used to prepare a calibration curve for urea detection.

d. For the urea spike and recovery study, milk and pH 4 buffer (Acetic acid-Sodium acetate) are mixed in a 1:3 ratio. In this mixture, different urea concentrations (0mM, 10mM, 20mM, 30mM, 50mM, 70mM, 100mM

and 200mM) are introduced. 100µl from every mixture is transferred to a microplate. 15µl of freshly prepared 2mg/ml urease is added to every mixture. The reaction mixture was then allowed to incubate for 5 min at 30°C. After that, 10µl 10x diluted mTFP protein is added. 96 well plate was placed in a microplate reader to observe the fluorescence. The response time to get a stable signal for urea detection (that includes incubation time) was around 6 min. The observed fluorescence signal for different urea concentrations is used to predict the urea concentration. The predicted urea concentration and actual concentrations are compared to calculate % recovery, average accuracy and % error.

2.8.4. mTFP thin film preparation and sensing studies

To prepare a thin film for milk pH sensing as a point of care solution, 20% (w/v) Gelatine solution was prepared and heated until a clear and transparent solution appeared. 20% Glycerine (v/v) was added to the solution. Glycerine provides water repellent property to the thin film, showing good stability in water. After that, it was allowed to cool down for some time and added with 10% (v/v) 10x diluted mTFP. The mixture is transferred into a petri-dish and allowed to air dry at room temperature. After letting it dry completely, it is cut into small pieces.

A piece of the thin film was excited with 462nm light, and the emission wavelength was checked.

To observe the leaching of mTFP from a thin film, it is dipped in water for one second, and fluorescence is observed. This process was repeated until it started showing a stable signal.

For milk pH sensing, a calibration curve is prepared. For this purpose, the thin film is dipped in the buffers of different pH, and then fluorescence intensity is observed. The spike and recovery study is done using these calibration curves in milk samples. The photostability of the thin film is observed for ten days.

3. Chapter 3 Results and discussion

3.1. Synthesis of carbon quantum dots

During the heating process, the solution undergoes a colour change. The clear and transparent solution turned into yellow-orange colour. This colour change is an indication of the successful synthesis of CQDs.

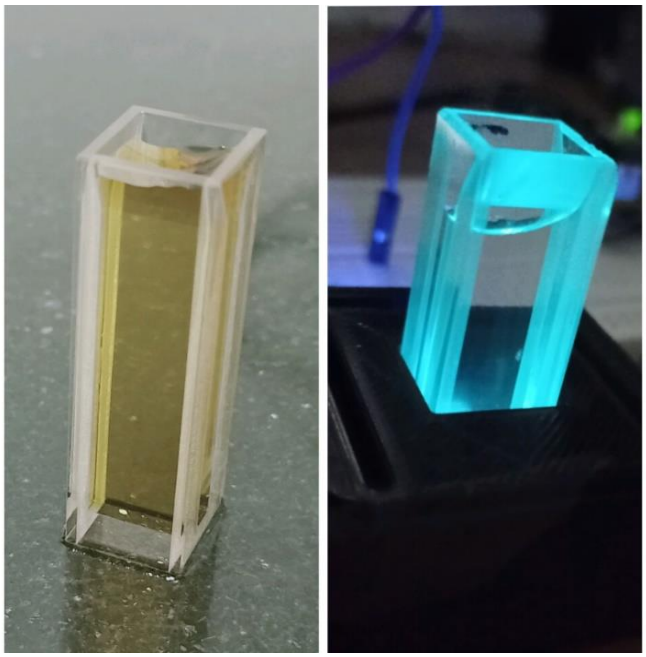

Figure 3.1 (a) CQDs under normal light (b) CQDs under UV light

3.2. Characterization of synthesized CQDs

A UV-vis spectrometer's absorption spectra of CQD solution showed a maximum absorption peak at 365 nm. The emission spectrum of the CQD solution was recorded using the OFS instrument, which showed the emission peak at 505nm. An XRD scan was taken in the range of 10-80º. The XRD pattern of CQDs shows the characteristic carbon-centred peak at 2θ =18°(Figure 5). This value of 2θ indicates a plane with a d spacing of 0.49 nm (using Bragg's equation). The broad pattern of the diffraction peak indicates the presence of nanoscale-sized CQDs. The XRD spectrum was compared with the previously reported CQDs and was found similar. XRD peak at 18° is the specification of highly amorphous carbon, while two minor peaks about 48° and 58° indicate the presence of low graphitic

carbon[41]. FTIR analysis was done to identify functional groups in lyophilized CQD powder and its precursor compounds- Phthalic acid and TED. Samples were scanned in a wavenumber range of 1000-4000cm^{-1}. Phthalic acid showed a broad peak around 3460cm^{-1} due to O-H bond stretching. The spectrum of TED showing peaks around 3500 cm^{-1} are due to N-H bond stretching. Synthesized CQD FTIR spectrum shows peaks 3300cm^{-1} to 3500cm^{-1} are due to O-H, and N-H bond stretching indicates the presence of O-H and N-H bonds. Peaks around 1500cm^{-1} show the presence of amide and carbon chains (Figures 4 and 5).

The quantum yield of the synthesized carbon dots was found to be 0.24 or 24%.

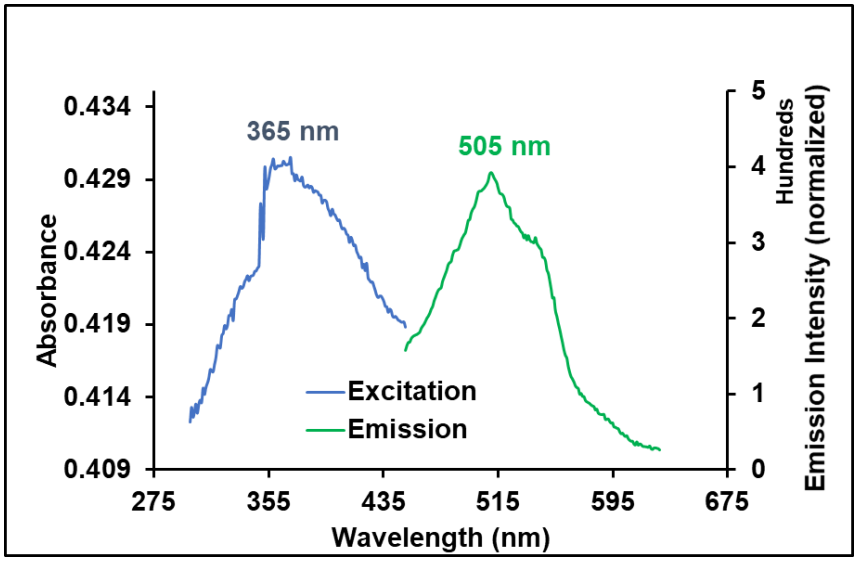

Figure 3.2 Optical properties of CQDs

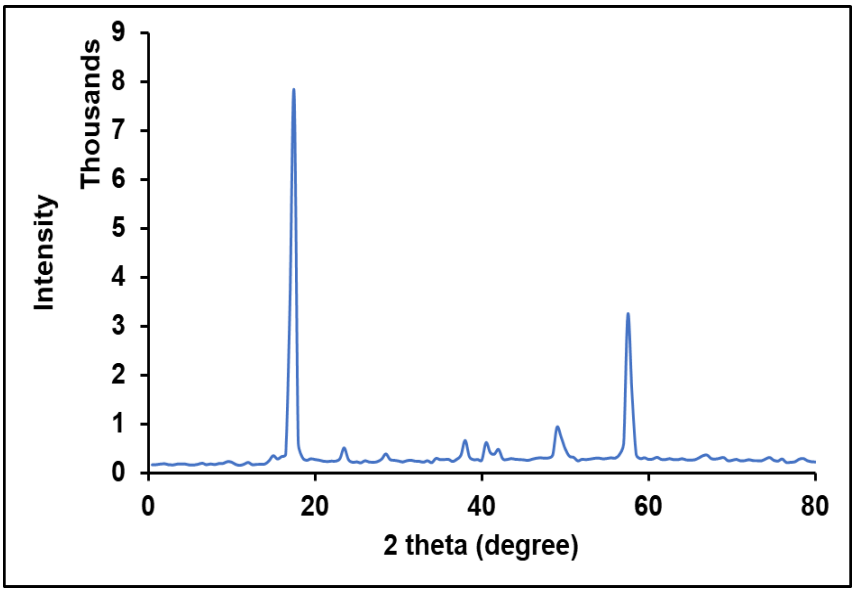

Figure 3.3 XRD spectrum of synthesized CQDs

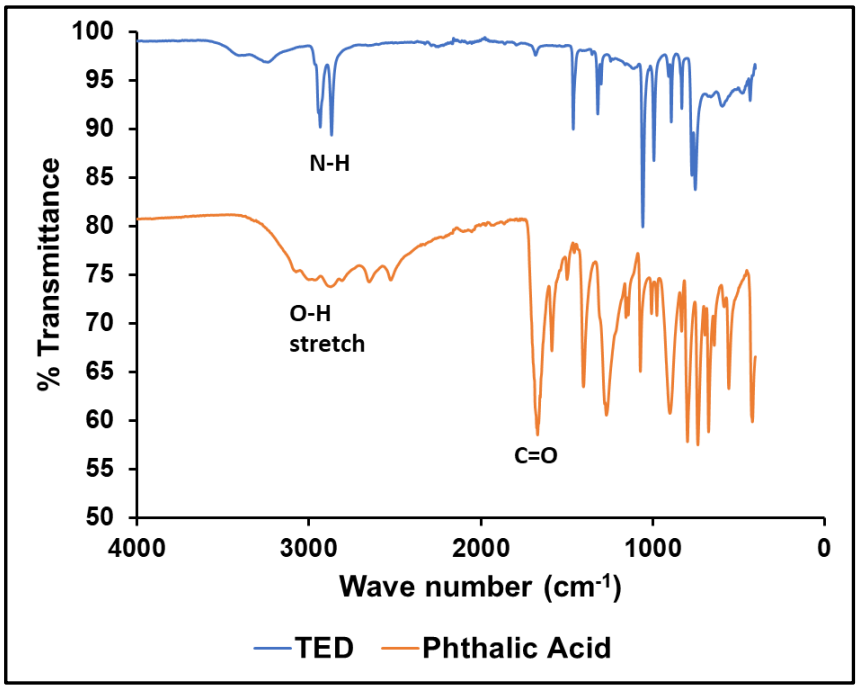

Figure 3.4 FTIR spectrum of TED and Phthalic acid

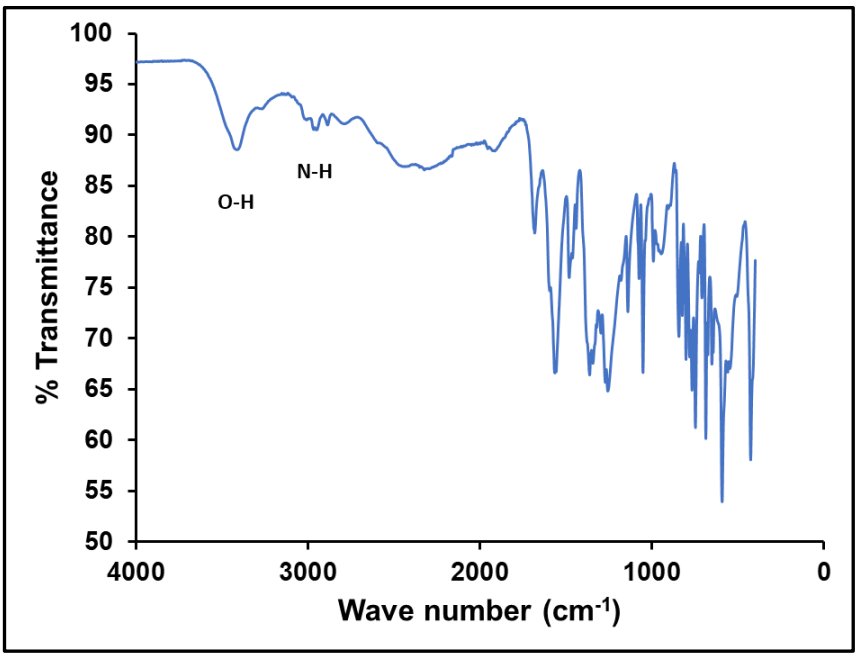

Figure 3.5 FTIR spectrum of synthesized CQDs

3.3. Photostability of CQDs

The CQD solution shows good photostability for 22 days. So, the synthesized carbon dots can be stored and used for a long duration without affecting their fluorescence. CQD is a suitable candidate for the application that requires stable fluorescent elements at higher temperatures.

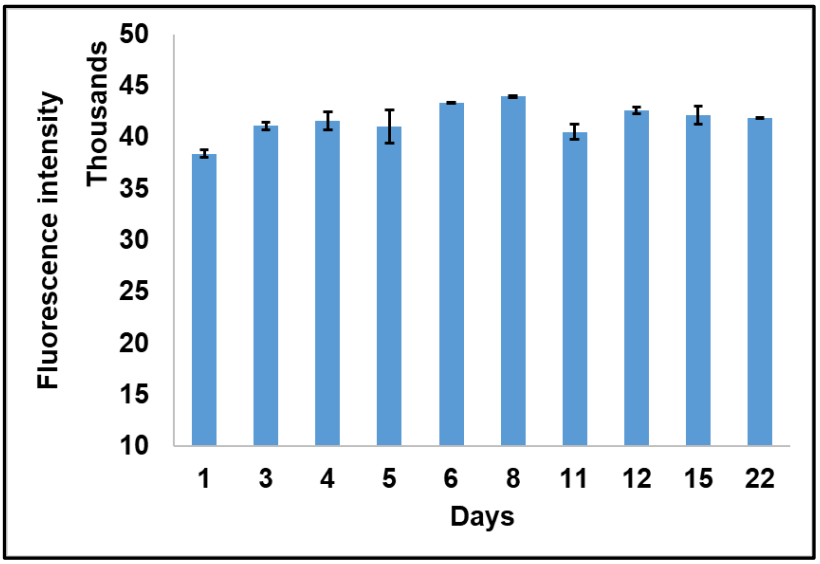

Figure 3.6 Photostability of CQD solution

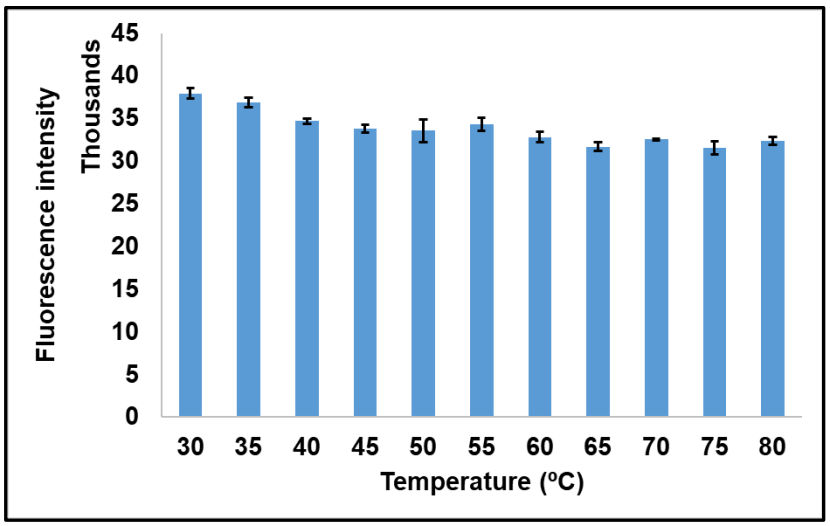

Figure 3.7 CQD fluorescence at different temperatures

3.4. Heavy metal ion sensing by CQDs

3.4.1. Preparation of calibration curves

The synthesized CQDs showed sensitivity for all concentrations of heavy metal salt solutions (range 0-100µM). A linear relation was observed between the concentration of heavy metal ions and the fluorescence intensity of CQDs. With the increase in concentration, more quenching was observed as the fluorescence intensity decreed. This relation can detect the heavy metal ion concentration in water. The relation for heavy metal ions was checked with parameters like linearity, limit of detection, limit of quantification, resolution and sensitivity.

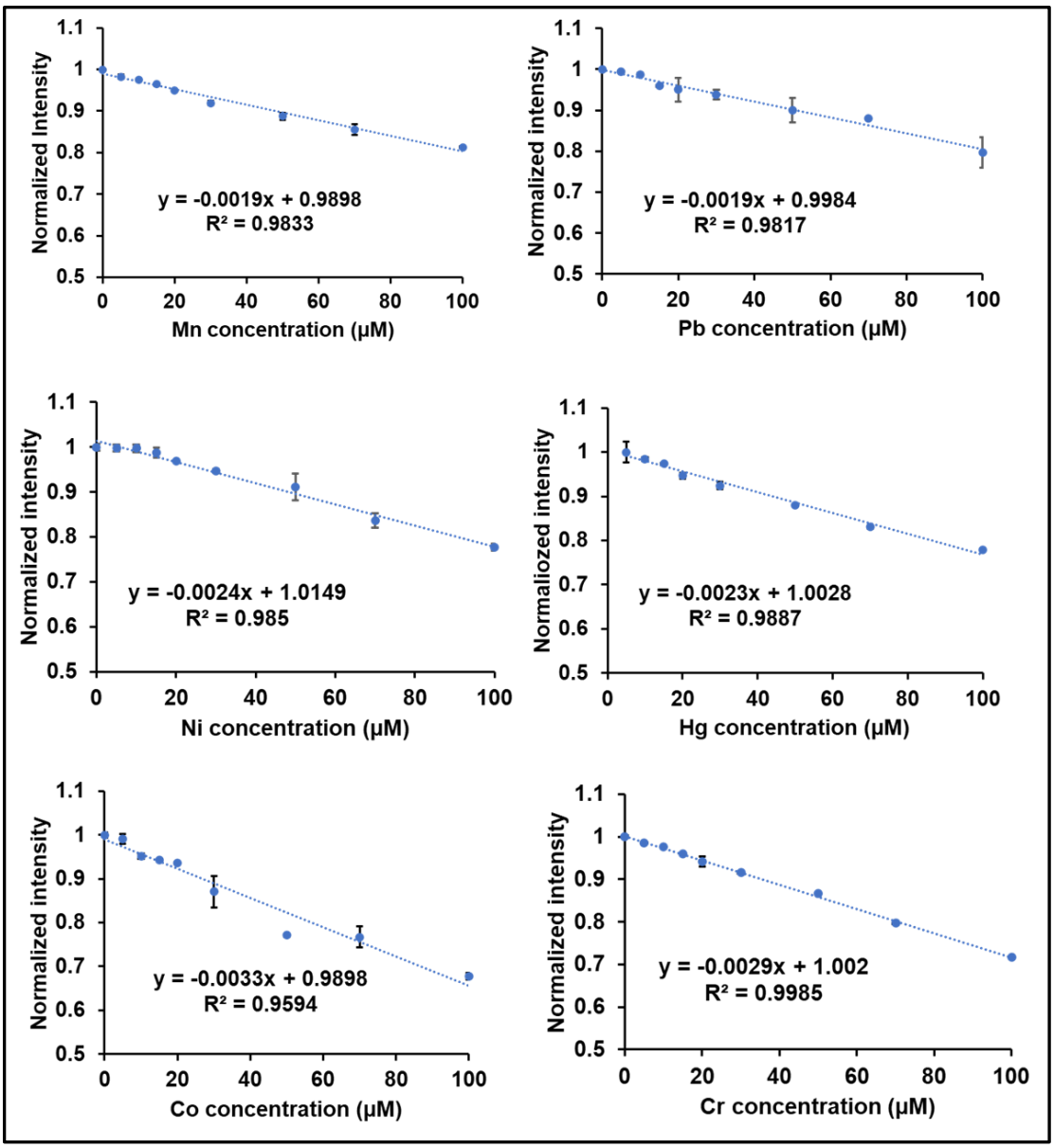

Figure 3.8 Calibration curves for different heavy metal ions

Table 3.0.1 Analysis of calibration curves

S.N.	Analytical parameter	Values					
		Mn	**Pb**	**Ni**	**Co**	**Hg**	**Cr**
1.	Linearity	0.983	0.981	0.985	0.959	0.988	0.998
2.	Sensitivity	0.0019 units/µM	0.0019 units/µM	0.0024 units/µM	0.0033 units/µM	0.0023 units/µM	0.0029 units/µM

3.	Limit of detection	0.052 µM	2.310 µM	10.68 µM	1.48 µM	2.883 µM	1.467 µM
4.	Limit of quantification	0.156 µM	6.931 µM	32.061µM	4.44 µM	8.651 µM	4.40 µM
5.	Resolution	0.0158 µM	0.700 µM	3.238 µM	0.448 µM	0.873 µM	0.444 µM

As the table shows, the lowest LOD and LOQ observed were for Manganese, and the highest LOD and LOQ observed were for Nickel.

3.4.2. Spike and recovery studies

Spike and recovery studies showed that the calibration curves could predict the heavy metal ion concentration. Observations for some heavy metal ions show that the lower value of the recovery range was slightly lower, and the upper value was slightly higher than the acceptable range of 85-100% as good. However, the mean recovery for all concentrations was around 100. The maximum average error value was around 10% for Mercury. Figure 9 shows graphs for spike and recovery studies, and table 3 shows the recovery range, mean recovery % and average error values for different heavy metal ions.

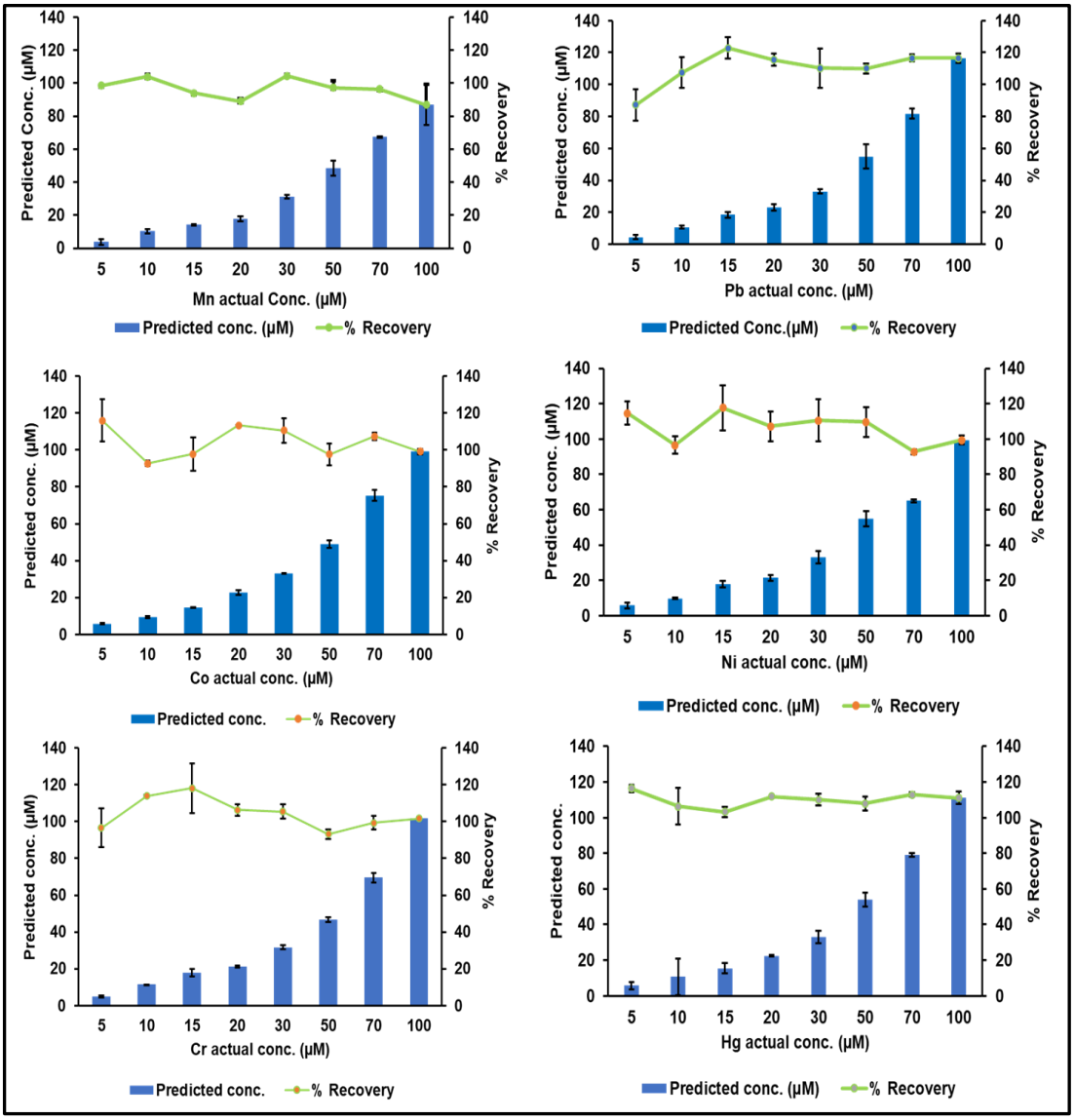

Figure 3.9 Spike and recovery experiments with CQDs (solution phase)

Table 3.0.2 Recovery results of different calibration curves

Parameters	Values					
	Hg	**Mn**	**Pb**	**Ni**	**Co**	**Cr**
Recovery range (%)	103.78-116.42	76.59-116.42	87.32-122.77	92.79-117.60	92.70-116.04	93.24-113.97
mean recovery (%)	110.01	93.54	110.79	106.05	104.33	104.34
Average % error in recovery	10.01	6.46	10.79	6.05	4.33	4.34

3.5. Synthesis and characterization of thin film

The synthesized thin film showed the fluorescent property. When excited with 365nm light, it showed the maximum emission peak at 498nm. All sensing studies were performed by exciting the thin film with 365nm light capturing the emission signal at 498nm.

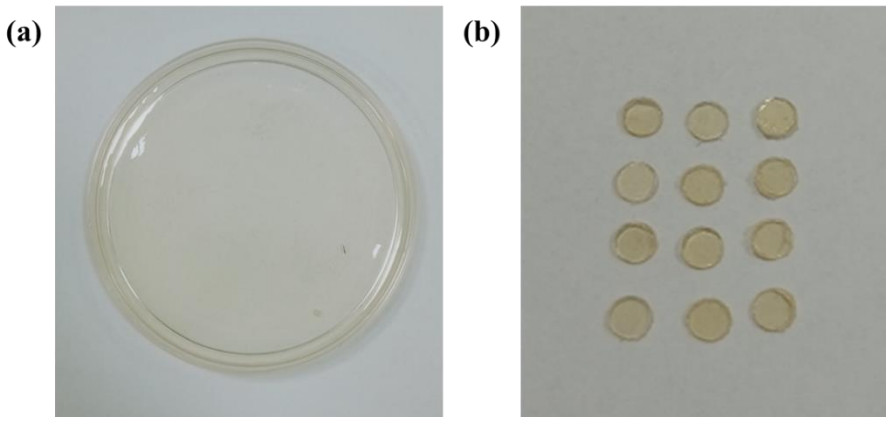

Figure 3.10 (a) Gelatin thin film in a petri dish (b) Small pieces of thin-film after cutting

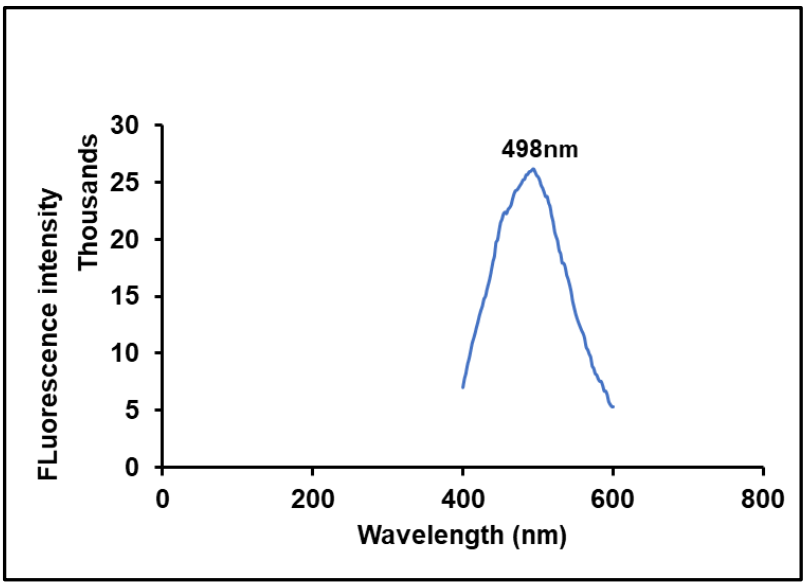

Figure 3.11 Fluorescence emission spectrum of CQD thin film

FTIR spectrum shows the characteristic peak of carbon dots (around 3400 cm^{-1}), which means that the chemical nature of carbon dots is not changed during the synthesis of the thin film. The functional groups responsible for the fluorescence of carbon dots are intact in the thin film.

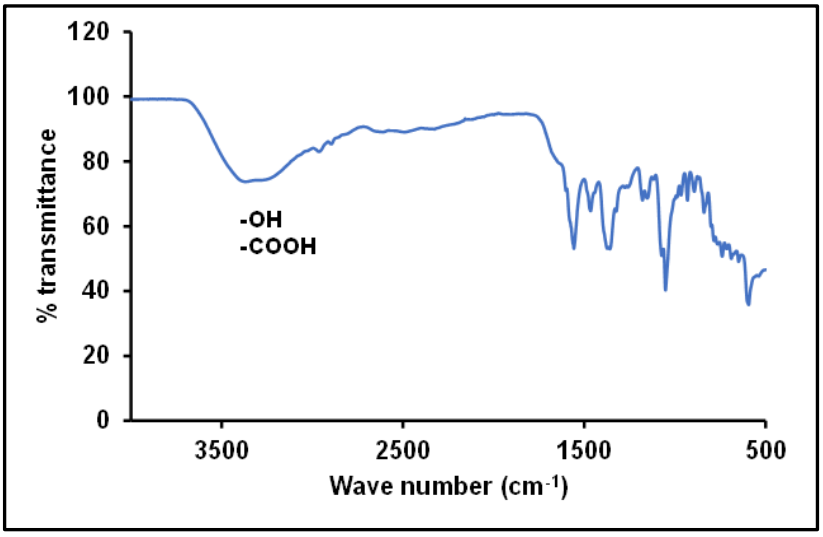

Figure 3.12 FTIR spectrum of the thin film

The XRD spectrum contains the characteristic peak of carbon dots (about 19.5º), which means that the crystal structure of carbon dots is changed during the preparation of the thin film. 2 theta value is 19.5º, which gives the d space value 0.46nm by Bragg's law.

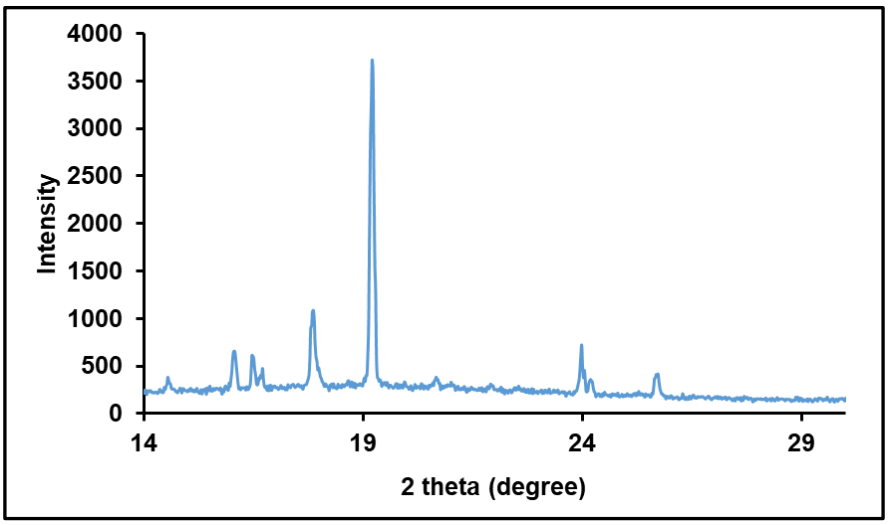

Figure 3.13 XRD spectrum of the thin film

The thin film showed excellent photostability as its fluorescence signal intensity remained similar for three weeks. It can be stored for a longer duration without affecting its accuracy.

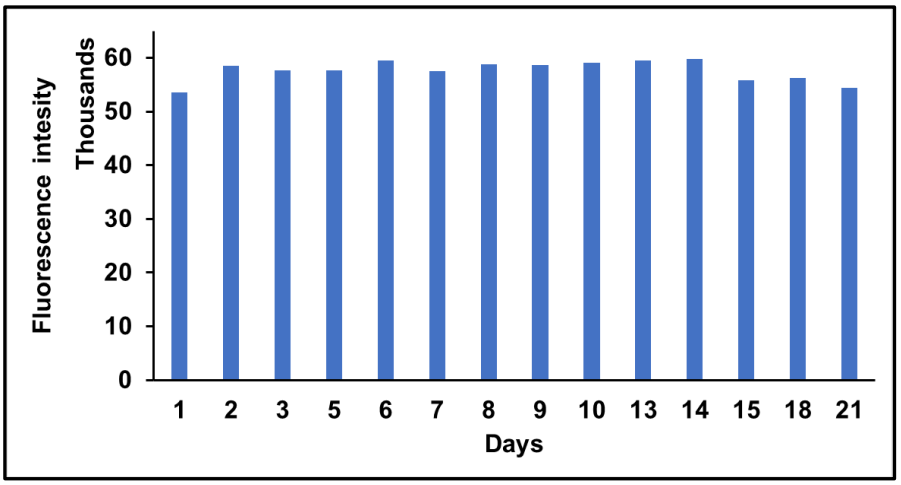

Figure 3.14 Photostability of CQD containing gelatin thin film

The thin film releases loosely bound carbon dots when dipped in water. Dipping it for two seconds is considered one cycle. After three cycles or six seconds, it started giving a stable signal which means that the loose bound carbon dots present on the surface were leached out. After three cycles, the signal intensity comes only due to inner bound carbon dots. The sensing experiments with the thin film are done before dipping the thin film in distilled water for about six seconds.

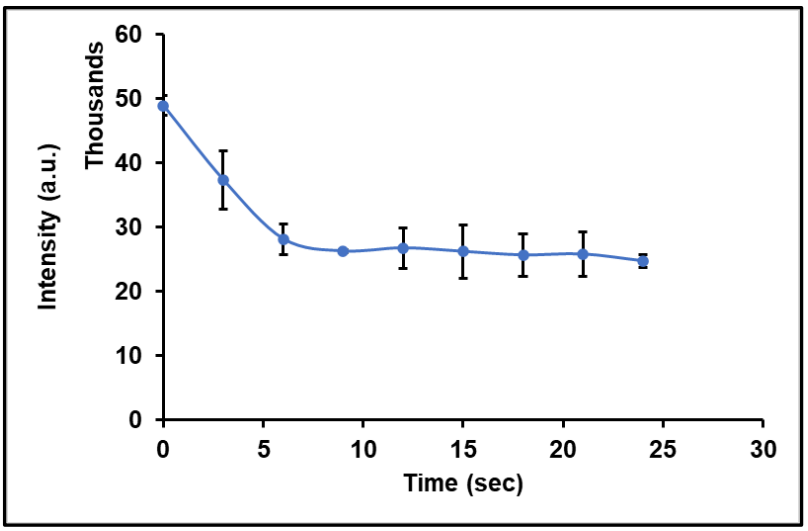

Figure 3.15 leaching of carbon dots from a thin film.

3.6. Sensing studies with thin film

Calibration curves were prepared to check the quenching pattern, and then spike and recovery experiments were done to check the validity of the calibration curves.

3.6.1. Preparation of calibration curves

Calibration curves were prepared for all six heavy metal ions (Hg, Ni, Co, Cr, Pb and Mn). They showed a linear relationship between concentration and fluorescence intensity.

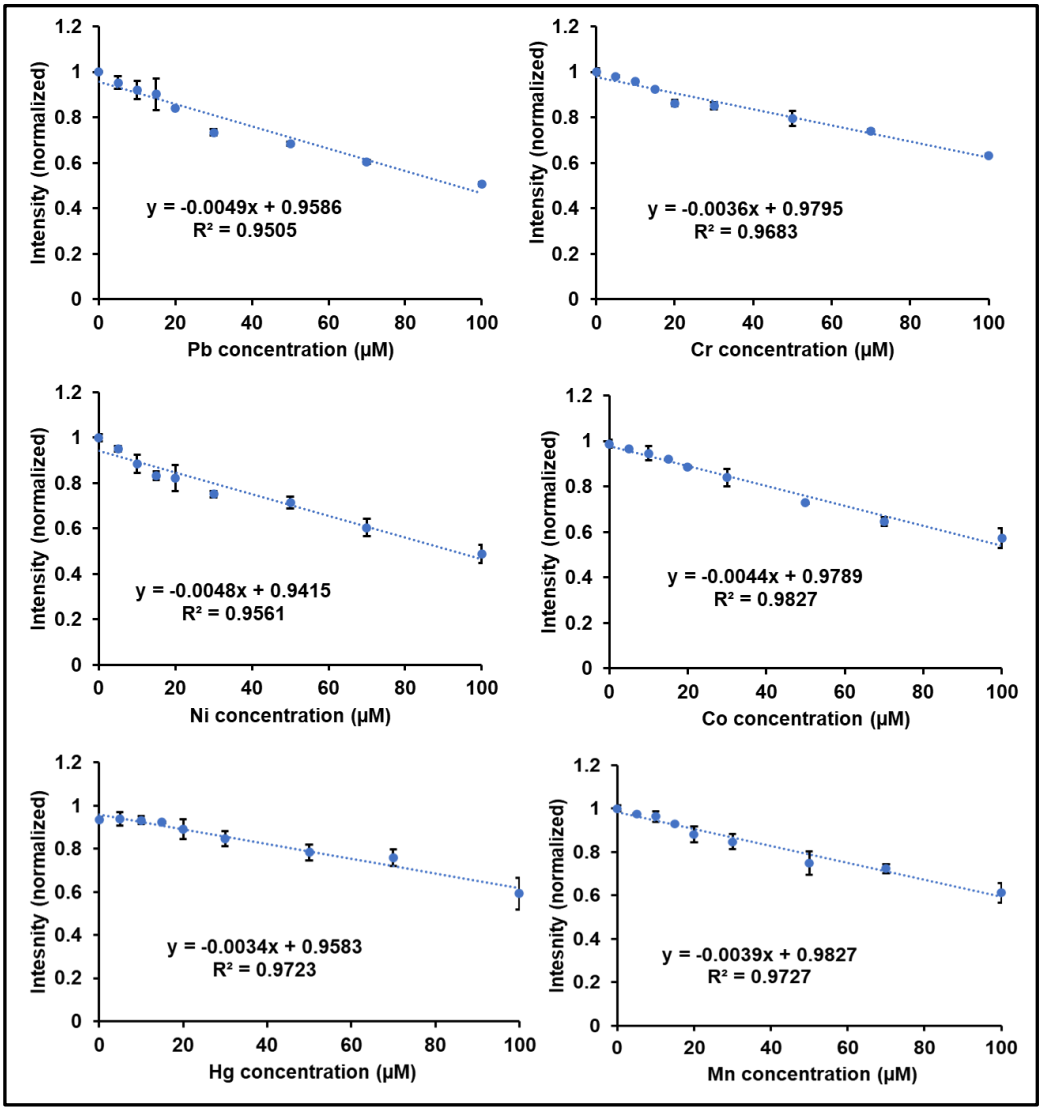

Figure 3.16 Calibration curves for sensing heavy metal ions with CQD thin film

3.6.2. Analysis of calibration curves

Table 4 analyses the calibration curves in terms of linearity, sensitivity, resolution, LOD and LOQ.

Table 3.0.3 Analysis of calibration curves prepared with CQDs thin film

S.N.	Analytical parameter	Values					
		Mn	Pb	Ni	Co	Hg	Cr
1.	Linearity	0.9727	0.9505	0.9561	0.9827	0.9723	0.9683

2.	Sensitivity	0.0039 units/µM	0.0049 units/µM	0.0048 units/µM	0.0044 units/µM	0.0034 units/µM	0.0036 units/µM
5.	Resolution	0.24 µM	0.6 µM	2.68 µM	0.55 µM	0.93 µM	1.11 µM
3.	Limit of detection	0.80 µM	1.98 µM	8.84 µM	1.80 µM	3.07 µM	3.63 µM
4.	Limit of quantification	2.4 µM	5.94 µM	26.52	5.4 µM	9.21 µM	10.89 µM

As the table shows, the lowest LOD and LOQ observed were for Manganese, and the highest LOD and LOQ observed were for Nickel (same as the solution phase).

3.6.3. Spike and recovery experiments

The validity of calibration curves is checked by spiking heavy metal ion concentration in tap water and then observing the quenching pattern. The predicted concentration is compared with calibration curves, and % recovery is calculated.

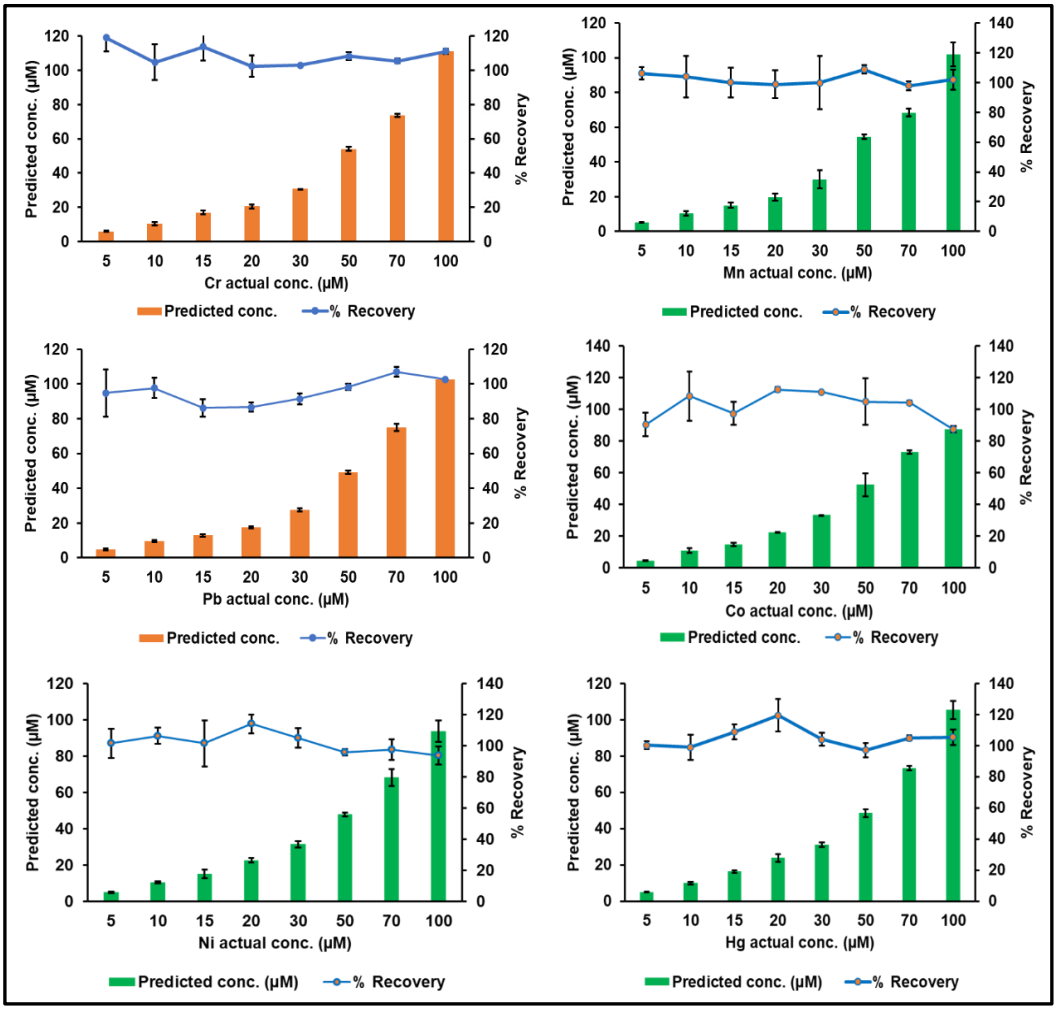

Figure 3.17 Spike and recovery experiments with thin film

3.6.4. Analysis of spike and recovery experiments

The thin film is capable of predicting the heavy metal ion concentration with a good % recovery. Table 5 is the analysis of spike and recovery experiments on different parameters.

Table 3.4 Analysis of spike and recovery experiments with thin film

Parameters	Values					
	Hg	Mn	Pb	Ni	Co	Cr
Recovery (%)	104.77	102.15	95.61	102.04	102.10	108.40
SD in % recovery	5.18	8.50	4.38	7.01	6.28	4.73
% Error (average)	4.77	2.15	4.39	2.04	2.10	8.40

3.7. Milk sensing studies

Recombinant mTFP was induced and purified, and milk sensing studies were done. pH calibration curves were prepared, and a pH spike and recovery study was done. For urea detection also, a calibration curve was prepared, and a spike and recovery study was performed. mTFP containing gelatin thin film was prepared as a rapid and accurate pH detection method.

3.7.1. Expression and purification mTFP

After induction with 0.1mM IPTG for 16hrs at 20°C, supernatant and pallet were run on 12% SDS gel. Gel image (figure 10a) shows that protein induction was in both fractions, pellet and supernatant. The soluble fraction or supernatant contains around 60-70% of the induced protein. A meagre fraction of mTFP in flow-through indicates that most mTFP molecules attach with Ni-NTA resin. A fraction of total protein appears in the elution lane (figure 10b). The protein eluted with 300mM imidazole was used for experiments.

a.

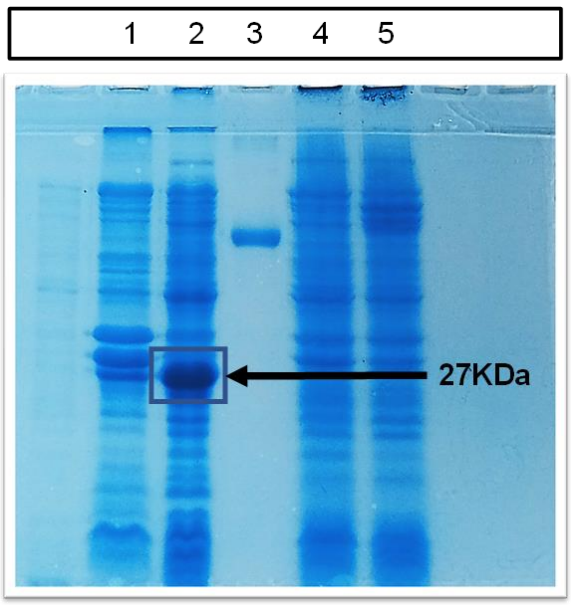

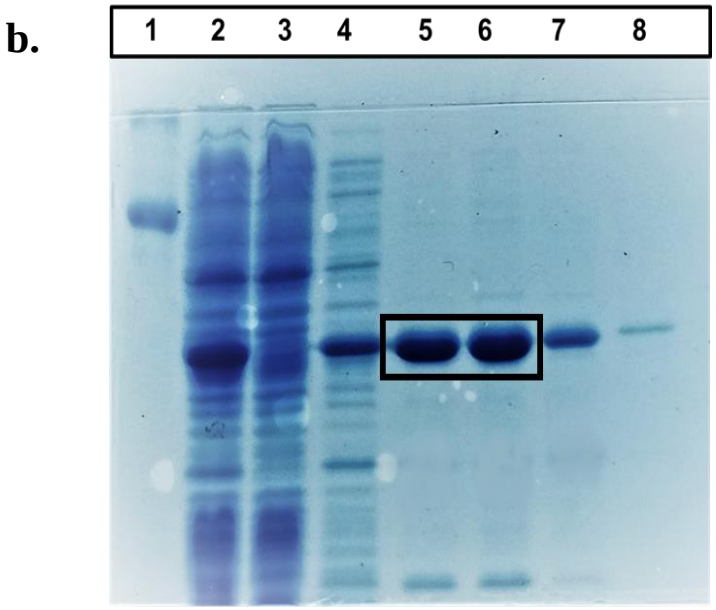

Figure 3.18 Gel image (a) Induction of recombinant mTFP lane 1: induced pellet, lane 2: induced supernatant, lane 3: 5mg BSA, lane 4: uninduced pellet, lane 5: uninduced supernatant

(b) lane 1: 5mg BSA, lane 2: input/lysate, lane 3: flow-through, lane 4: 50mM imidazole wash, lane 5: 300mM imidazole first elution, lane 6: second elution

3.7.2. Milk pH sensing with mTFP (solution phase)

mTFP showed a linear relationship between its fluorescence and pH. In the pH range from 3.5 to 6.5, the fluorescence intensity increases with the increase in the pH. This relationship is used to prepare a pH calibration curve that is further utilized to detect the pH of the milk. The regression coefficient of the calibration curve was found to be more than 0.95, and the relationship can be considered linear.

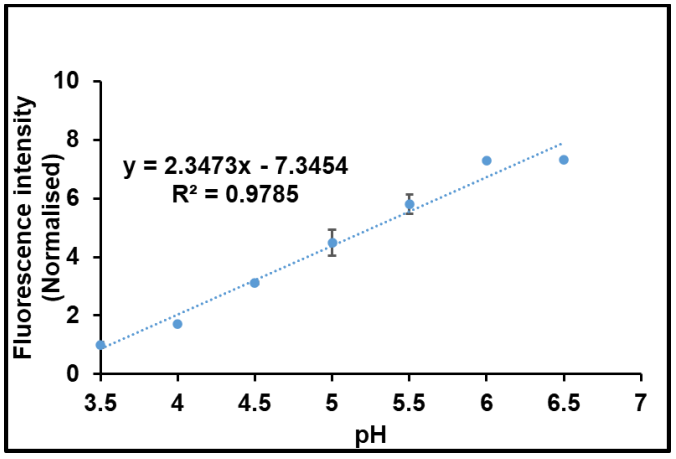

Figure 3.19 Calibration curve for milk pH detection

In pH spike and recovery studies, the results showed that the calibration curve is valid for detecting the milk pH. All points of pH values showed good recovery with mTFP. The selected pH range was 3.5 to 6.5, covering the pH change during natural spoilage. During natural spoilage, the pH of milk can fall up to 4. The average % recovery in this study was 95%, with an average error of 5%.

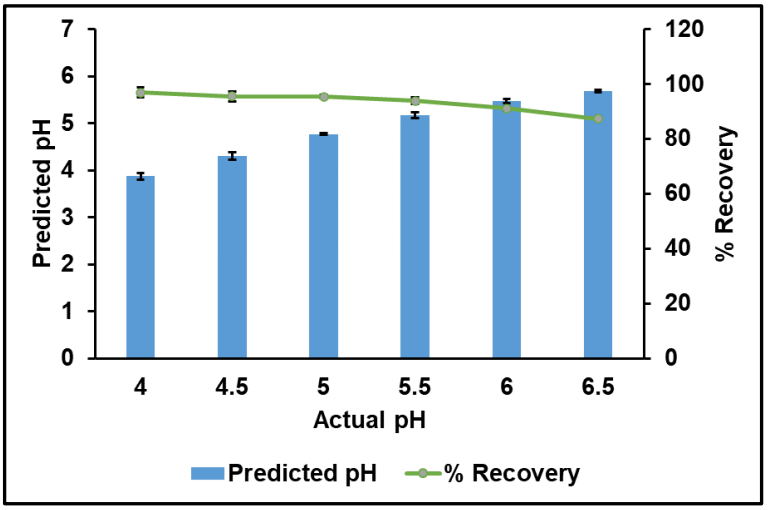

Figure 3.20 pH spike and recovery study with mTFP

3.7.3. Urea sensing with mTFP (solution phase)

A. During urea-urease reactions, the ammonium ions are responsible for increasing the pH. Hence, pH and urea (with urease) concentration show a linear relationship.

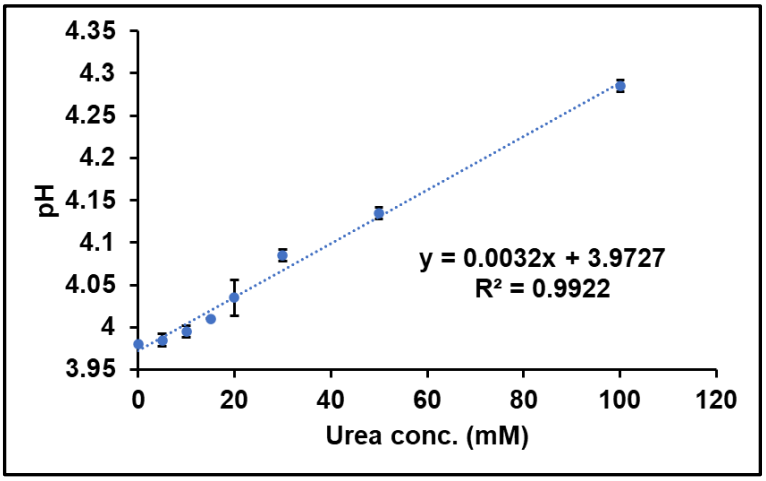

Figure 3.21 relationship between urea (with urease) concentration and pH

B. Due to an increase in the pH, the fluorescence intensity of mTFP also increases with urea concentration. Figure 23 is the calibration curve for

urea sensing.

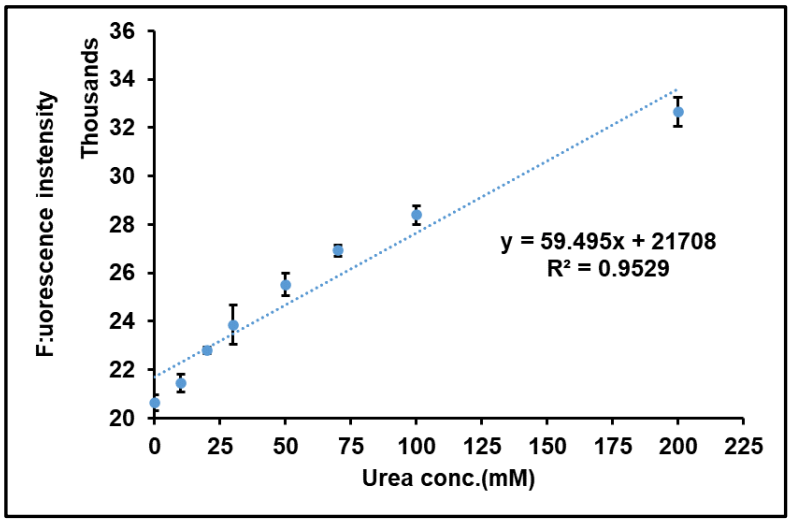

Figure 3.22 Calibration curve for urea detection in milk

C. In the urea concentration range 0-100mM, this calibration showed good % recovery and predicted the urea concentration with acceptable accuracy.

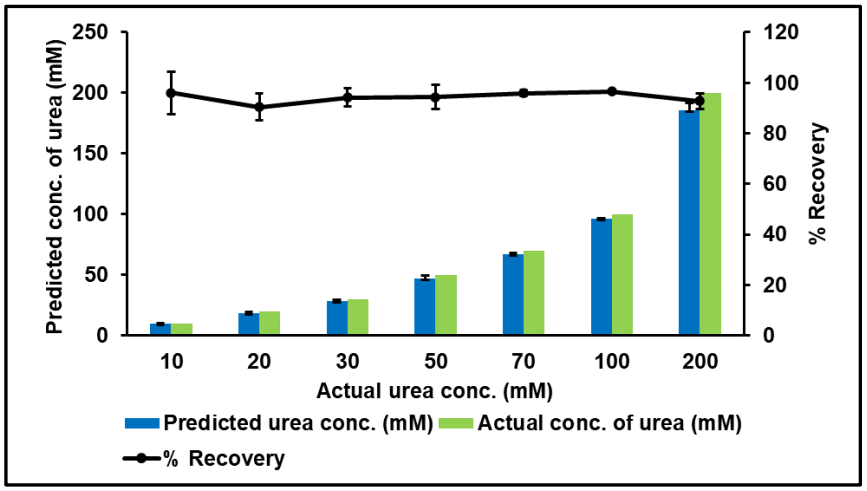

Figure 3.23 Urea spike and recovery experiment

- As a part of the control experiment and to check if urea (without urease) is affecting the fluorescence of mTFP or not, the fluorescence intensity is checked with different urea concentrations. The reaction volume and mTFP volume were kept for all urea concentrations during the experiment. The results showed that the urea present in milk did not affect the fluorescence of mTFP. (also, the pH of different urea concentrations remains the same)

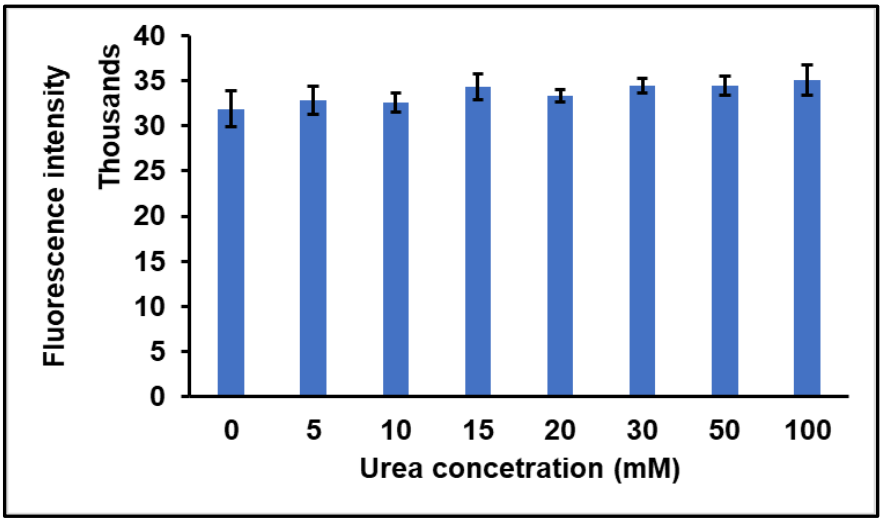

Figure 3.24 Effect of urea fluorescence of mTFP

3.7.4. mTFP thin film synthesis and milk pH sensing

Synthesized gelatin thin film showed fluorescence property. When excited with 462nm light, it showed maximum emission at 497nm. For further studies, 462nm and 497nm lights are used as excitation and emission wavelengths.

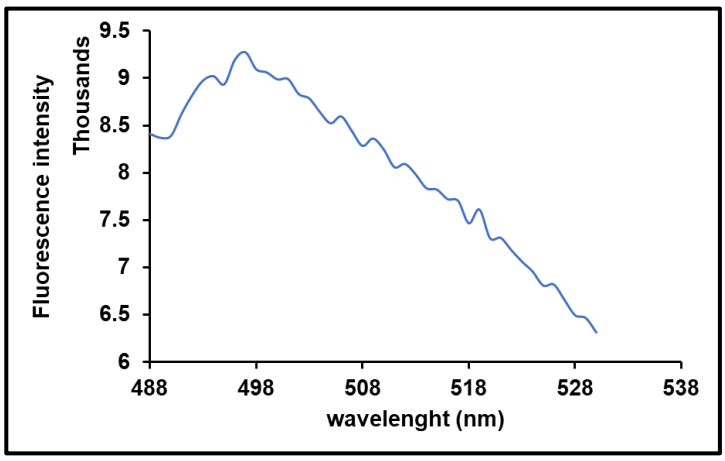

Figure 3.25 Fluorescence emission spectra of mTFP thin film

When dipped in water to check the leaching of mTFP from thin, it is observed that after three cycles or three seconds, it started giving a stable signal. So for further studies, the mTFP thin film is dipped in water for 3 seconds before taking observations to ensure that any change in the fluorescence is due to pH only.

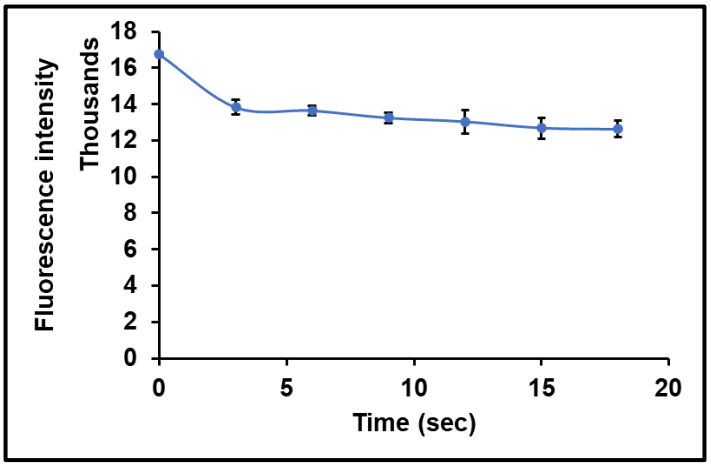

Figure 3.26 leaching of mTFP from gelatin thin film

The thin film showed pH sensitivity in the pH range of 3.5 to 6.5 (same as the solution phase). Using the observed fluorescence intensity, the pH calibration curve is prepared for sensing studies in milk.

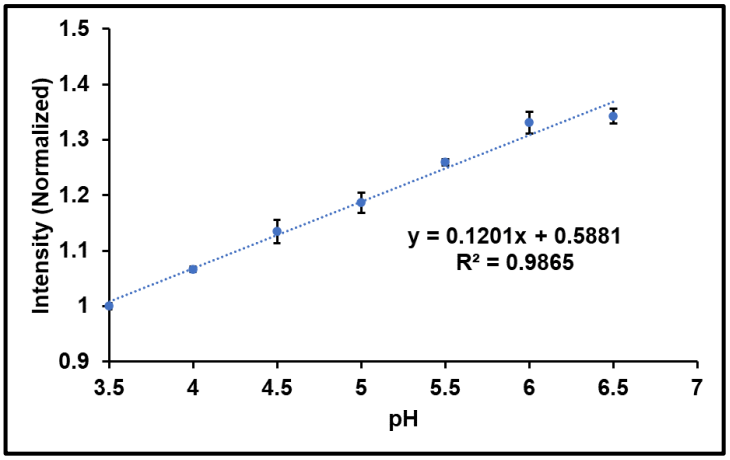

Figure 3.27 Calibration curve for milk pH sensing with mTFP thin film

In pH spike and recovery studies, the calibration curve was found to be valid for milk pH detection and able to predict the milk pH with acceptable accuracy.

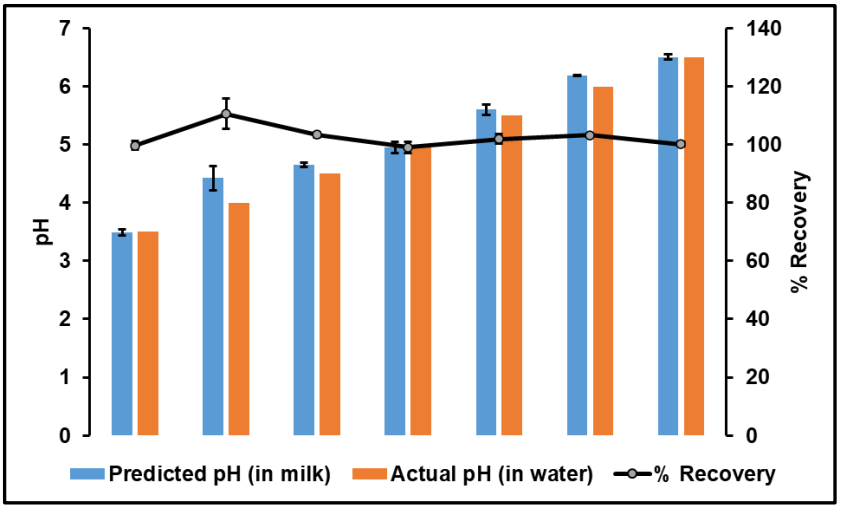

Figure 3.28 pH spike and recovery experiments with mTFP thin film

The average % recovery in spike and recovery experiments was 102.54%, with an average error of 5%. The results showed that thin-film based pH detection has excellent accuracy and can be considered for milk pH sensing purposes.

4. Chapter 4 Conclusion and future aspects

For the first objective of this study (heavy metal ion sensing in water), CQDs were synthesized and characterized. The characterization results were compared with the previously reported studies and found similar. Fluorescence quenching studies for Lead, Nickel, Mercury, Cobalt, Chromium and Manganese were done for detection purposes. All the calibration curves showed the linear regression pattern in the concentration range of 0-100µM. Spike and recovery studies for these heavy metal ions were done to check the usability/validity of calibration curves. The known concentration of the metal ions was spiked in the solution, and CQD fluorescence was checked. Fluorescence intensity for the known concentration was used to predict the heavy metal ion concentration. This predicted value was compared with the actual value. All the calibration curves are able to show the recovery in the decent range.

A CQDs embedded thin film is a ready-to-use and easy solution for detecting heavy metal ions in water. For that purpose, A carbon dot embedded thin film is synthesized with gelatin. For extra stability in water, glycerine was mixed during its preparation. The synthesized thin film showed good photostability and fluorescence property. Calibration curves for all six heavy metal ions (Lead, Nickel, Mercury, Cobalt, Chromium and Manganese) were prepared. The spike and recovery experiments were repeated with the thin film.

The results showed that the thin film is able to detect the heavy metal ions (Lead, Nickel, Mercury, Cobalt, Chromium and Manganese) with decent accuracy.

For the second objective of this study (sensing natural spoilage and urea adulteration in milk), recombinant mTFP was induced and purified. This recombinant protein showed a pH-sensitive property. A calibration curve for pH range 3.5 to 6.5 was prepared. This calibration was used for pH spike and recovery studies of milk spoilage. mTFP protein detected the urea in the concentration range 0-200mM, covering the acceptable urea concentration in milk (9mM-11mM). mTFP embedded thin film showed pH sensitivity, same as solution phase. pH spike and recovery studies showed thin film's excellent accuracy and usability.

To extend this study, dual fluorophore based matrices can be developed to be more accurate and specific to a particular heavy metal ion. The combination of fluorophores will give a unique signal for every heavy metal ion.

5. Chapter 5 References

1. Geissen V, Mol H, Klumpp E, et al. Emerging pollutants in the environment: a challenge for water resource management. *International soil and water conservation research*. 2015;3(1):57-65. doi: 10.1016/j.iswcr.2015.03.002

2. Kalyoncu L, Kalyoncu H, Arslan G. Determination of heavy metals and metals levels in five fish species from Işıklı Dam Lake and Karacaören Dam Lake (Turkey). *Environmental monitoring and assessment*. 2012;184(4):2231-2235. doi: 10.1007/s10661-011-2112-9

3. Duruibe JO, Ogwuegbu MOC, Egwurugwu JN. Heavy metal pollution and human biotoxic effects. *International Journal of physical sciences*. 2007;2(5):112-118.

4. Bagal-Kestwal D, Karve MS, Kakade B, Pillai VK. Invertase inhibition based electrochemical sensor for the detection of heavy metal ions in aqueous system: Application of ultra-microelectrode to enhance sucrose biosensor's sensitivity. *Biosensors and Bioelectronics*. 2008;24(4):657-664. doi:10.1016/j.bios.2008.06.027

5. Turdean GL. Design and Development of Biosensors for the Detection of Heavy Metal Toxicity. *International Journal of Electrochemistry*. 2011;2011:e343125. doi:10.4061/2011/343125

6. Tag K, Riedel K, Bauer HJ, Hanke G, Baronian KHR, Kunze G. Amperometric detection of Cu2+ by yeast biosensors using flow injection analysis (FIA). *Sensors & Actuators: B Chemical*. 2007;2(122):403-409. doi:10.1016/j.snb.2006.06.007

7. Gumpu MB, Sethuraman S, Krishnan UM, Rayappan JBB. A review on detection of heavy metal ions in water – An electrochemical approach. *Sensors and Actuators B: Chemical*. 2015;213:515-533. doi:10.1016/j.snb.2015.02.122

8. Singh R, Gautam N, Mishra A, Gupta R. Heavy metals and living systems: An overview.
Indian J Pharmacol. 2011;43(3):246. doi:10.4103/0253-7613.81505

9. Rajaganapathy V, Xavier F, Sreekumar D, Mandal PK. Heavy metal contamination in soil, water and fodder and their presence in livestock and products: a review. *Journal of Environmental Science and technology*. 2011;4(3):234-249.

10. Vogl J, Heumann KG. Determination of heavy metal complexes with humic substances by HPLC/ICP-MS coupling using on-line isotope dilution technique. *Fresenius' Journal of Analytical Chemistry*. 1997;359(4-5):438-441. doi:10.1007/s002160050606

11. Senapati T, Senapati D, Singh AK, Fan Z, Kanchanapally R, Ray PC. Highly selective SERS probe for Hg(II) detection using tryptophan-protected popcorn shaped gold nanoparticles. *Chem Commun*. 2011;47(37):10326-10328. doi:10.1039/C1CC13157E

12. Bernaus A, Gaona X, Esbrí JM, Higueras P, Falkenberg G, Valiente M. Microprobe Techniques for Speciation Analysis and Geochemical Characterization of Mine Environments: The Mercury District of Almadén in Spain. *Environ Sci Technol*. 2006;40(13):4090-4095. doi:10.1021/es052392l

13. Kunkel Robert, Manahan SE. Atomic absorption analysis of strong heavy metal chelating agents in water and waste water. *Anal Chem*. 1973;45(8):1465-1468. doi:10.1021/ac60330a024

14. Metters JP, Kadara RO, Banks CE. Electroanalytical sensing of chromium(III) and (VI) utilizing gold screen printed macro electrodes. *Analyst*. 2012;137(4):896-902. doi:10.1039/C2AN16054D

15. Gogoi N, Barooah M, Majumdar G, Chowdhury D. Carbon Dots Rooted Agarose Hydrogel Hybrid Platform for Optical Detection and Separation of Heavy Metal Ions. *ACS Appl Mater Interfaces*. 2015;7(5):3058-3067. doi:10.1021/am506558d

16. Shimizu FM, Braunger ML, Riul A. Heavy metal/toxins detection using electronic tongues. *Chemosensors*. 2019;7(3):36. doi: 10.3390/chemosensors7030036

17. Strianese M, Staiano M, Ruggiero G, Labella T, Pellecchia C, D'Auria S. Fluorescence- Based Biosensors. In: Bujalowski WM, ed. *Spectroscopic Methods of Analysis*. Vol 875. Methods in Molecular Biology. Humana Press; 2012:193-216. doi:10.1007/978-1-61779-806-1_9

18. Valizadeh A, Mikaeili H, Samiei M, et al. Quantum dots: synthesis, bioapplications, and toxicity. *Nanoscale Research Letters*. 2012;7(1):480. doi:10.1186/1556-276X-7-480

19. Xue B, Yang Y, Sun Y, Fan J, Li X, Zhang Z. Photoluminescent lignin hybridized carbon quantum dots composites for bioimaging applications. *International Journal of Biological Macromolecules*. 2019;122:954-961. doi:10.1016/j.ijbiomac.2018.11.018

20. Fan H, Zhang M, Bhandari B, Yang C hui. Food waste as a carbon source in carbon quantum dots technology and their applications in food safety detection. *Trends in Food Science & Technology*. 2020;95:86-96. doi:10.1016/j.tifs.2019.11.008

21. Xu X, Ray R, Gu Y, et al. Electrophoretic Analysis and Purification of Fluorescent Single-Walled Carbon Nanotube Fragments. *J Am Chem Soc*. 2004;126(40):12736- 12737. doi:10.1021/ja040082h

22. Sun YP, Zhou B, Lin Y, et al. Quantum-Sized Carbon Dots for Bright

and Colorful Photoluminescence. *J Am Chem Soc*. 2006;128(24):7756-7757. doi:10.1021/ja062677d

23. Dager A, Uchida T, Maekawa T, Tachibana M. Synthesis and characterization of Mono- disperse Carbon Quantum Dots from Fennel Seeds: Photoluminescence analysis using Machine Learning. *Sci Rep*. 2019;9(1):14004. doi:10.1038/s41598-019-50397-5

24. Fei X, Gu Y. Progress in modifications and applications of fluorescent dye probe.
Progress in Natural Science. 2009;19(1):1-7.
doi:10.1016/j.pnsc.2008.06.004

25. Saud PS, Pant B, Alam AM, Ghouri ZK, Park M, Kim HY. Carbon quantum dots anchored TiO2 nanofibers: Effective photocatalyst for waste water treatment. *Ceramics International*. 2015;41(9, Part B):11953-11959. doi:10.1016/j.ceramint.2015.06.007

26. Luo PG, Sahu S, Yang ST, et al. Carbon "quantum" dots for optical bioimaging. *J Mater Chem B*. 2013;1(16):2116-2127. doi:10.1039/C3TB00018D

27. Wang W, Li Y, Cheng L, Cao Z, Liu W. Water-soluble and phosphorus-containing carbon dots with strong green fluorescence for cell labeling. *J Mater Chem B*. 2013;2(1):46-48. doi:10.1039/C3TB21370F

28. Wu H, Zeng F, Zhang H, Xu J, Qiu J, Wu S. A Nanosystem Capable of Releasing a Photosensitizer Bioprecursor under Two-Photon Irradiation for Photodynamic Therapy. *Advanced Science*. 2016;3(2):1500254. doi:10.1002/advs.201500254

29. Ding H, Du F, Liu P, Chen Z, Shen J. DNA–Carbon Dots Function as Fluorescent Vehicles for Drug Delivery. *ACS Appl Mater Interfaces*. 2015;7(12):6889-6897. doi:10.1021/acsami.5b00628

30. Nair A, Haponiuk JT, Thomas S, Gopi S. Natural carbon-based quantum dots and their applications in drug delivery: A review. *Biomed Pharmacother*. 2020;132:110834. doi:10.1016/j.biopha.2020.110834

31. Basu A, Suryawanshi A, Kumawat B, Dandia A, Guin D, Ogale SB. Starch (Tapioca) to carbon dots: an efficient green approach to an on-off-on photoluminescence probe for fluoride ion sensing. *Analyst*. 2015;140(6):1837-1841. doi:10.1039/C4AN02340D

32. Tyagi A, Malika Tripathi K, Singh N, Choudhary S, Kumar Gupta R. Green synthesis of carbon quantum dots from lemon peel waste: applications in sensing and photocatalysis. *RSC Advances*. 2016;6(76):72423-72432. doi:10.1039/C6RA10488F

33. Ying Lim S, Shen W, Gao Z. Carbon quantum dots and their applications. *Chemical Society Reviews*. 2015;44(1):362-381.

doi:10.1039/C4CS00269E

34. Rani UA, Ng LY, Ng CY, Mahmoudi E. A review of carbon quantum dots and their applications in wastewater treatment. *Advances in Colloid and Interface Science*. 2020;278:102124. doi:10.1016/j.cis.2020.102124

35. Devi P, Rajput P, Thakur A, Kim KH, Kumar P. Recent advances in carbon quantum dot- based sensing of heavy metals in water. *TrAC Trends in Analytical Chemistry*. 2019;114:171-195. doi:10.1016/j.trac.2019.03.003

36. Zhu S, Song Y, Zhao X, Shao J, Zhang J, Yang B. The photoluminescence mechanism in carbon dots (graphene quantum dots, carbon nanodots, and polymer dots): current state and future perspective. *Nano Res*. 2015;8(2):355-381. doi:10.1007/s12274-014-0644-3

37. Lakowicz JR, ed. Quenching of Fluorescence. In: *Principles of Fluorescence Spectroscopy*. Springer US; 2006:277-330. doi:10.1007/978-0-387-46312-4_8

38. Wang Y, Hu A. Carbon quantum dots: synthesis, properties and applications. *J Mater Chem C*. 2014;2(34):6921-6939. doi:10.1039/C4TC00988F

39. M. Lu, Y. Shiau, J. Wong, R. Lin, H. Kravis, T. Blackmon, T. Pakzad, T. Jen, A. Cheng, J. Chang, E. Ong, N. Sarfaraz and N. Wang, "Milk Spoilage: Methods and Practices of Detecting Milk Quality," *Food and Nutrition Sciences*, Vol. 4 No. 7A, 2013, pp. 113-123. doi: 10.4236/fns.2013.47A014.

40. Marcus Y. Chin, Anand R. Patwardhan, Kean-Hooi Ang, Austin L. Wang, Carolina Alquezar, Mackenzie Welch, Phi T. Nguyen, Michael Grabe, Anna V. Molofsky, Michelle R. Arkin, Aimee W. Kao. "A genetically encoded, pH-sensitive mTFP1 biosensor for probing lysosomal pH". bioRxiv 2020.11.04.368654; doi: https://doi.org/10.1101/2020.11.04.368654.

41. Hou H, Banks CE, Jing M, Zhang Y, Ji X. Carbon "Quantum Dots and Their Derivative 3D Porous Carbon Frameworks for Sodium-Ion Batteries with Ultralong Cycle Life". *Advanced Materials*. 2015;27(47):7861-7866. doi:10.1002/adma.201503816